OSTBAYERISCHE TECHNISCHE HOCHSCHULE REGENSBURG

ELEKTRO- UND INFORMATIONSTECHNIK

Linear Feedback Loops

Prof. Dr. Martin J. W. Schubert

Electronics Laboratory

Ostbayerische Technische Hochschule Regensburg

Regensburg, Bavaria, Germany

Linear Feedback Loops

Abstract. Linear feedback loop models are introduced.

1 Introduction

1.1 Simple Model

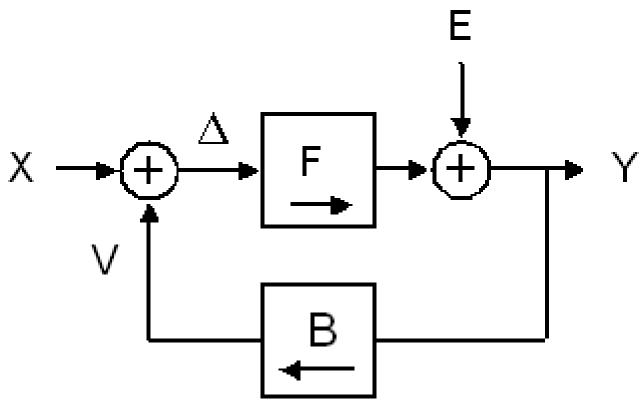

Fig. 1.1: Basic model of linear feedback loop including output error *E*.
.

The feedback loop model in Fig. 1.2.2.1 with *F* and *B* being linear and time-invariant (LTI) models in *s* or *z* features signal transfer function (*STF*) and noise transfer function (*NTF*)

$$STF = \left.\frac{Y}{X}\right|_{E=0} = \frac{F}{1+FB} \xrightarrow{|FB|\to\infty} B^{-1} \tag{1.1.1}$$

$$NTF = \left.\frac{Y}{E}\right|_{X=0} = \frac{1}{1+FB} \xrightarrow{|FB|\to\infty} 0 \tag{1.1.2}$$

To derive *STF* according to (1.1.1) set *E*=0 (corresponding to a short circuit) so that

$$Y = F \cdot \Delta = F(X-V) = F(X-BY) = FX - FBY \;\;\rightarrow\;\; Y(1+FB) = FX \;\;\Leftrightarrow\;\; \frac{Y}{X} = \frac{F}{1+FB}\,.$$

Exercise: To derive (1.1.2) do the same derivation with input signal *E* and *X*=0:

$Y = F\varepsilon + E =$ ....

Important goals and features of this loop are:
- High loop amplification |*FB*| given, then:
- Loop inverts transfer function of feedback network *B*,
- Error entries behind forward network F are suppressible
- Errors of feedback network *B* are not suppressible (loop can never be better than *B*!),
- Input errors such as input noise of input offset of the op-amp are unsurpassable “input”

Note that we have calculated with frequency-domain functions. Expressions like *Y=STF·X* in frequency domain correspond to a convolution (deutsch: Faltung) in time-domain, according to

$y(t) = h_{STF}(t)*x(t)$ with $h_{STF}(t)$ being the impulse response of the *STF* and the '*' operator standing for convolution.

Exercise 1.1:
Compute the amplification *STF=Y/X* of the System in Fig. 1.1(a) for *F*=10000, *B*=1/10.
Compute the noise suppression *NTF=Y/E* o f the System in Fig. 1.1(a) for *F*=10000, *B*=1/10.

Solution 1.1: $STF = 10^4/(1+0.1\cdot10^4) = 9.99$, $NTF = 1/(1+0.1\cdot10^4) = 9.99\cdot10^{-4}$.

Exercise 2 (for *Matlab* users):
Using *Matlab's LTI* systems [1] created by `tf(…)` the behavior of a feedback loop as illustrated in Fig. 1.1(a) is modeled with command `feedback`. Example:

Listing 1: Computing *STF* and *NTF* with Matlab for the system in Fig. 1

```
% Use Matlab's LTI functions to compute STF and NTF as feedback loops
F = tf(1E4)            % Forward network amplification
B = tf(0.1)            % Backward network amplification
STF = feedback(F,B)    % build STF as LTI system
NTF = feedback(1,F*B)  % build NTF as LTI system
```

1.2 More Advanced Modelling

Fig. 1.2: Basic model of linear feedback loop including Input error E_X and output error E.
.

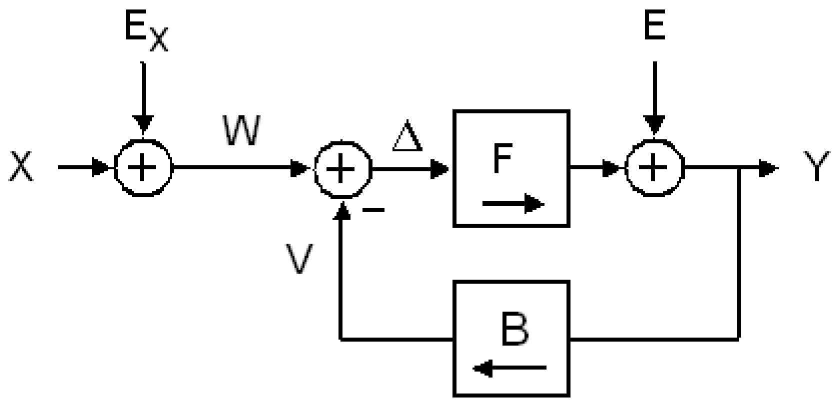

The feedback loop in Fig. 1.2 is modeled as

$$Y = F \cdot \Delta + E = F(W - V) + E = F\big((X + E_X) - B \cdot Y\big) + E = F(X + E_X) - F \cdot B \cdot Y + E\,.$$

Rearrangement delivers $$Y = \frac{F(X + E_X) + E}{1 + FB}\,. \tag{1.2.1}$$

Sensitivity to input signal X: $$\frac{\partial Y}{\partial X} = STF = \frac{F}{1 + FB} \xrightarrow{|FB| \to \infty} B^{-1} \tag{1.2.2}$$

Sensitivity to input error E_X: $$\frac{\partial Y}{\partial E_X} = STF = \frac{F}{1 + FB} \xrightarrow{|FB| \to \infty} B^{-1} \tag{1.2.3}$$

Sensitivity to error E: $$\frac{\partial Y}{\partial E} = NTF = \frac{1}{1 + FB} \xrightarrow{|FB| \to \infty} 0 \tag{1.2.4}$$

Consequences:

1. Input error E_X is not suppressed by high loop gain, but is treated in exactly the same way as input signal X.

2. If B is erroneous, (1.2.3) remains valid. Consequently, if
$$B = B_{ideal}(1 + \varepsilon)\,,\ \varepsilon \ll 1 \quad \rightarrow \quad B^{-1} \cong B_{ideal}^{-1}(1 - \varepsilon)\,. \tag{1.2.5}$$

1.3 The organization of this document is as follows:

Section 1 presents in a very short form the basic feedback loop configuration and equations.
Section 2 presents 4 axioms of *linear and time invariant* (LTI) signal processing and appl.,
Section 3 extends loop topologies to higher order systems.
Section 4 explains filters canonic direct structures,
Section 5 illustrates translation from $s \rightarrow z$ domain,
Section 6 explains fundamentals concerning poles and zeros in transfer functions,
Section 7 is concerned with stability,
Section 8 details theory in several practical application examples,
Section 9 draws relevant conclusion and
Section 10 offers references.
Section 11 is an appendix used e.g. for detailed mathematical proofs.

2 Linearity and Time Invariance (LTI)

2.1 The 4 Axioms of Signal Processing

2.1.1 Linearity Axiom

$$y[\ c_1 \cdot x_1(t)\ +\ c_2 \cdot x_2(t)\ ]\ =\ c_1 \cdot y[\ x_1(t)\ ]\ +\ c_2 \cdot y[x_2(t)]. \tag{2.1}$$

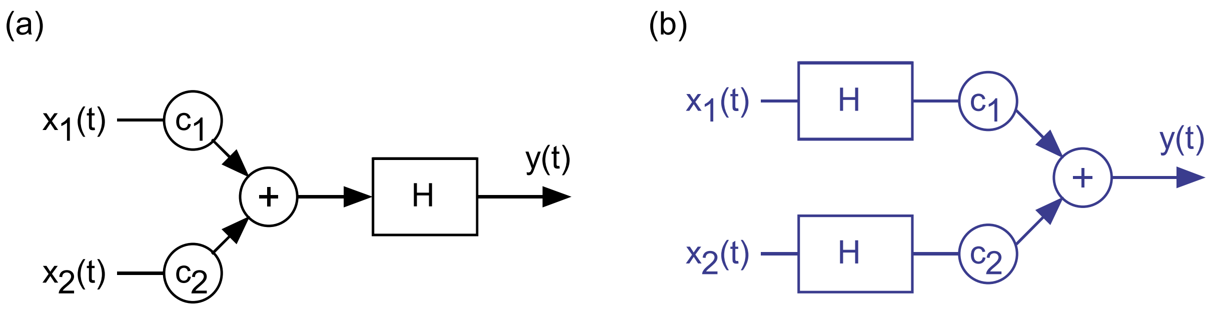

Fig. 2.1.1: (a) linear superposition of two signals, **(b)** equivalent system.

Linearity for signal processing systems is defined according equation (2.1), illustrated by Fig. 2.1.1.

Proportionality Implication.

Setting c_2=0 in equation (2.1) shows: Linearity implies proportionality:

$$y[\ c \cdot x(t)]\ =\ c \cdot y[x(t)] \tag{2.2}$$

as illustrated in Fig. 2.1.2. Proportionality allows to shift constants over LTI systems and therefore to combine several constants within the circuit mathematically to a single constant.

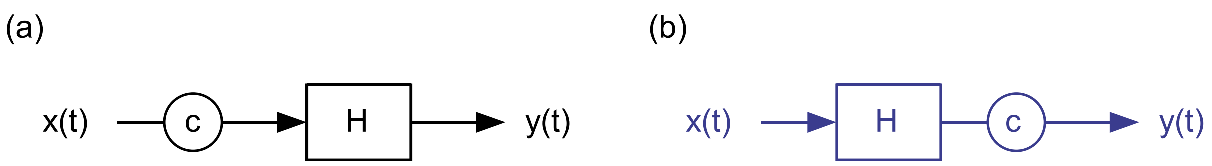

Fig. 2.1.2: Proportionality: Systems (a) and (b) are equivalent for linear circuits.

Zero-Offset Implication.

Setting c=0 in equation (2.2) shows: Proportionality implies zero offset:

$$y[0]\ =\ 0 \cdot y[x(t)]\ =\ 0 \tag{2.3}$$

Conclusion:
The resistive divider in Fig. 2.1.3(a) is linear, because U_2 = constant · U_1.
The circuit with operational amplifier in Fig. 2.1.3(b) is non-linear, as $U_2 \neq 0$ when U_1=0.

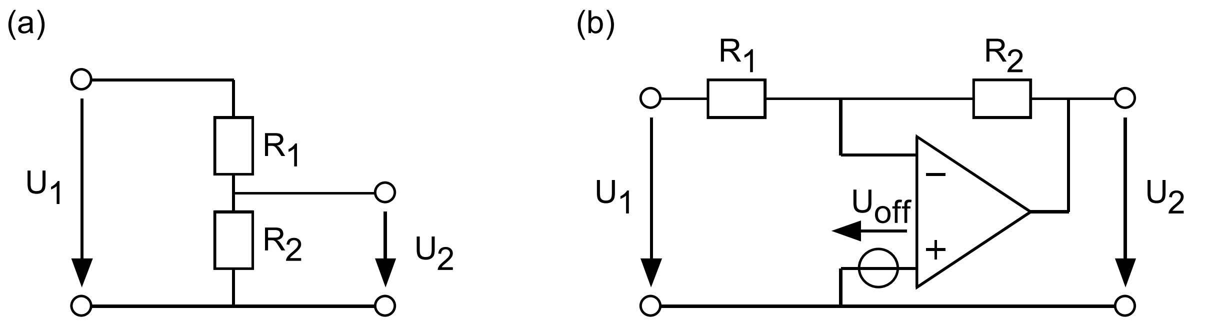

Fig. 2.1.3: (a) resistive divider, **(b)** circuit using OpAmp with offset voltage $U_{off} \neq 0$.

Remark: Linearity according to Eq. (2.1) is a signal processing definition. From a mathematical point of view a system $U_{out} = a \cdot U_{in} + b$ with constants a, b is linear.

2.1.2 Time Invariance Axiom

A system is time invariant when its impulse response $h(t)$ is not a function of time:

$$h(t) = h(t-\tau) \tag{2.4}$$

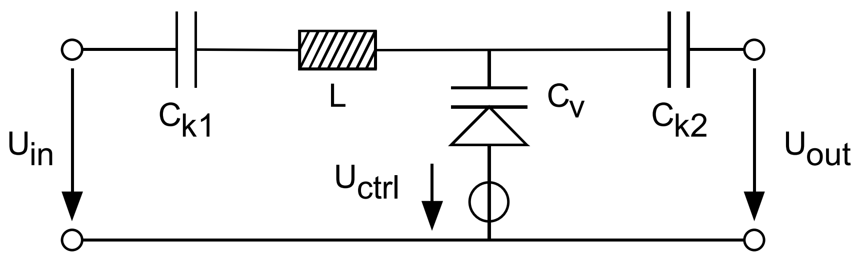

Fig. 2.1.4: Time-variant system when U_{ctrl} varies with time

Most systems we use are time-invariant. An example for a time-variant system is shown in Fig. 2.1.4, where response U_{out} to the impulses at U_{in} depends on control voltage U_{ctrl}, which varies with time.

2.1.3 Causality Axiom : $y(t) = f(x(\tau))$ with $\tau \leq t$

The present state of a system, $y(t)$, is a function of the past and present state of its input, but not of future inputs.

2.1.4 Stability Definition : Bounded Input Bounded Output (BIBO)

Definition: There exist constants M and K, so that from $|x(t)| \leq M$ follows $|y[x(t)]| \leq K \cdot M$.
Question: Is an ideal integrator BIBO stable? (Hint: consider $f \to 0$!)

2.2 Application LTI Axioms

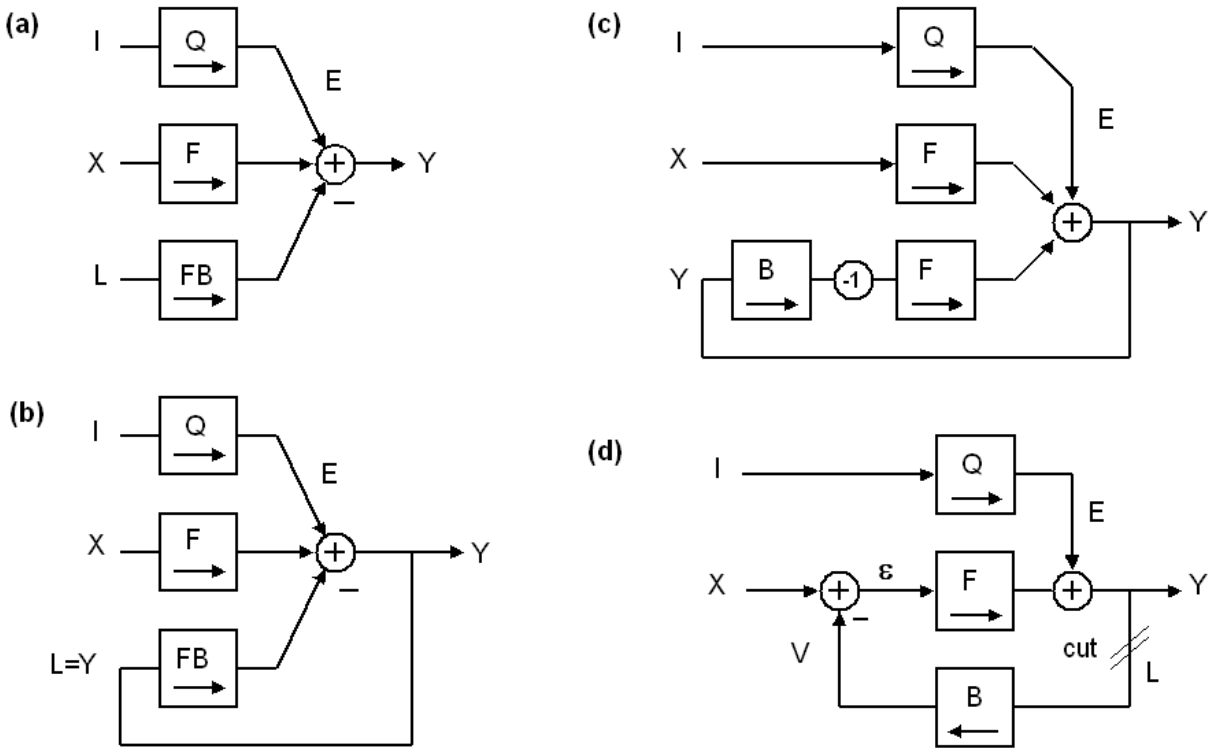

Fig. 2.2: Evaluation of the feedback loop equations.

In Fig. 2.2(a) the transfer function of the system is

$Y = Q{\cdot}I + F{\cdot}X - FB{\cdot}L$

In Fig. 2.2(b) from $L=Y$ follows $(1 + FB)\cdot Y = F{\cdot}X + Q{\cdot}I$ and consequently

$$Y = \frac{F}{1+FB}X + \frac{Q}{1+FB}I \quad = \quad STF \cdot X + NTF \cdot I \tag{2.5}$$

The so-called signal and noise transfer functions are

$$STF = \left.\frac{Y}{X}\right|_{E=0} = \frac{F}{1+FB} \xrightarrow{|FB|\to\infty} B^{-1}. \tag{2.6}$$

$$NTF = \left.\frac{Y}{I}\right|_{X=0} = \frac{Q}{1+FB} \xrightarrow{|FB|\to\infty} 0\,. \tag{2.7}$$

In Fig. 2.2(c) *FB* was split in $B{\cdot}F$. Proportionality allows moving factor -1 over network *F*.

In Fig. 2.2(d) Linearity allows to unify the 2 networks *F* without changing (2.6), (2.7).

Opening the Loop at "*cut*" in Fig. 2.2(d) allows to measure $Q{=}E/I$, $F{=}Y/X$ and $FB{=}Y/L$.

2.3 Positive Feedback

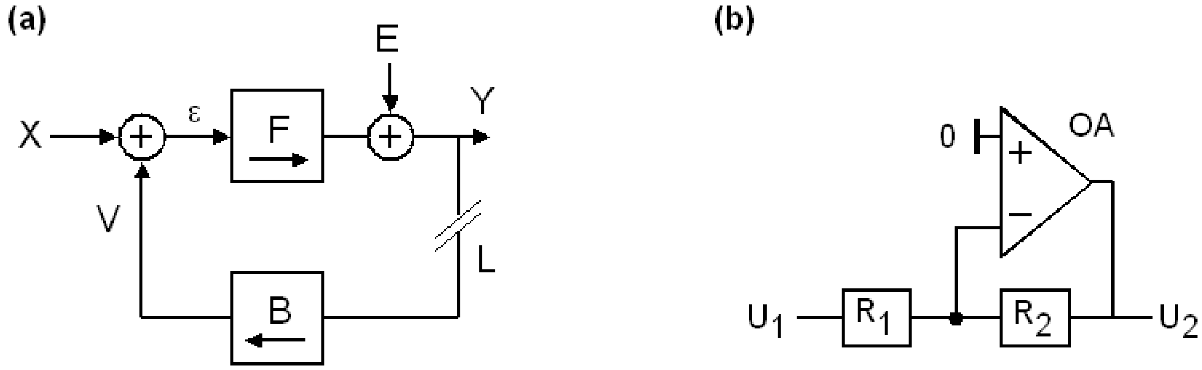

Fig. 2.3: (a) feedback branch *B* is fed back without negation at summation point, (b) example

In Fig. 2.3(a), the feedback is realized as summation without explicit negation at the summation point. Consequently, there must be a negation somewhere else in the loop to avoid oscillation. An application example is Fig. 2.3(b), where *OpAmp AO* in the forward network is inverting.

Fig. 2.3(a) delivers

$$Y = F\varepsilon = F(X+V) = F(X+BY) = FX + FBY \;\rightarrow\; Y(1-FB) = FX \;\Leftrightarrow\; \frac{Y}{X} = \frac{F}{1-FB}.$$

(Open) loop gain *FB* can be taken from

$$Y\big|_{E=0} = FB \cdot L \;\Leftrightarrow\; \left.\frac{Y}{L}\right|_{E=0} = FB \tag{2.8}$$

This delivers the signal and noise transfer functions

$$STF = \left.\frac{Y}{X}\right|_{E=0} = \frac{F}{1-FB} \xrightarrow{|FB|\to\infty} -B^{-1}. \tag{2.9}$$

Similarly, $X = 0$ and forward network 1 as $Y = E$ at open loop, we get

$$NTF = \left.\frac{Y}{E}\right|_{X=0} = \frac{1}{1-FB} \xrightarrow{|FB|\to\infty} 0. \tag{2.10}$$

Generalized strategy, suitable also for distributed feedback to compute the (open) loop gain:
- Cut the loop at any site in the feedback branch such that cutting a single wire opens the loop.
- Figure out the forward network $F = Y/X$ at E=0 and open loop,
- Figure out the (open) loop gain *FB* from one end of the cut to the other.
- With *F* and *FB* we can set up equations (2.9) and (2.10).

In this kind of loop phase margin is measured against -360° (not against -180°).

3 Network Topologies

Higher order systems often come in one of two topologies:

- Topology 1: distributed feed-in common network, concentrated feed-out,
- Topology 2: distributed feed-out of common network, concentrated feed-in.

3.1 Topology 1: Distributed Feed-In

3.1.1 Derivation

Fig. 3.1.1:

Distributed feed-in network

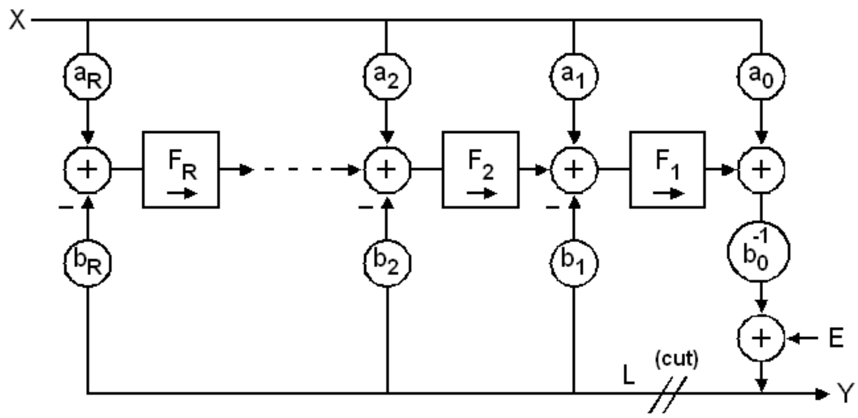

Open the loop at its concentrated point (*cut*) as shown in Fig. 3.1.1. Then determine the feed-forward network *F* by setting *L*=0. Identify any possible path from *X* to *Y*. In linear systems, solutions superpose linearly.

Feed Forward network of order *R*:

$$F = \left.\frac{Y}{X}\right|_{L=E=0} = \left[a_0 + a_1F_1 + a_2F_1F_2 + ... + a_RF_1F_2...F_R\right]\frac{1}{b_0}, \tag{3.1.1}$$

(Open) loop network of order *R*:

$$FB = \left.\frac{Y}{L}\right|_{X=E=0} = -\left[b_1F_1 + b_2F_1F_2 + ... + b_RF_1F_2...F_R\right]\frac{1}{b_0}$$

According to chapter 2.3, eq. ((2.9, (2.19), signal and noise transfer functions are obtained by closing the loop setting *L*=*Y* to deliver

$$STF = \left.\frac{Y}{X}\right|_{E=0} = \frac{F}{1-FB} = \frac{a_0 + a_1F_1 + a_2F_1F_2 + ... + a_RF_1F_2...F_R}{b_0 + b_1F_1 + b_2F_1F_2 + ... + b_RF_1F_2...F_R}\ , \tag{3.1.3}$$

$$NTF = \left.\frac{Y}{E}\right|_{X=0} = \frac{1}{1-FB} = \frac{b_0}{b_0 + b_1F_1 + b_2F_1F_2 + ... + b_RF_1F_2...F_R}\ , \tag{3.1.4}$$

In this network type input signal *X* passes the feed-forward filter defined by coefficients a_k, k=0…*R*, <u>before</u> it enters the feed-back loop. We have the chance to cancel or attenuate critical frequencies before they circulate in the feed-back loop.

3.1.2 Feedback Topology with *STF* = 1

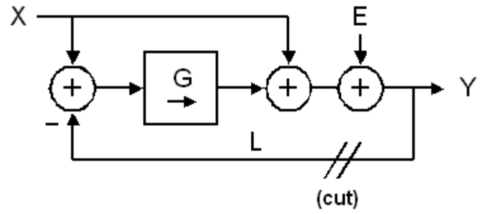

Fig. 3.1.2: Feedback Topology with *STF* = 1 and freedoms to shape the *NTF*.

Set in Fig. 3.1.1 $b_R = a_R = a_0 = 1$ and all other coefficients equal zero. To obtain Fig. 3.1.2. Let $G = F_1 \cdot \ldots \cdot F_{R\text{-}1}$. Then

$$STF = \frac{d_R \cdot G + d_0}{1 + b_R \cdot G} = \frac{1 \cdot G + 1}{1 + 1 \cdot G} = 1 \tag{3.1.5}$$

$$NTF = \frac{1}{1+G} \tag{3.1.6}$$

The signal transfer function is always ideally *STF*=1, i.e. flat over frequency and *G* can be used to shape noise by the *NTF*.

3.2 Topology 2: Distributed Feed-Out

3.2.1 Derivation

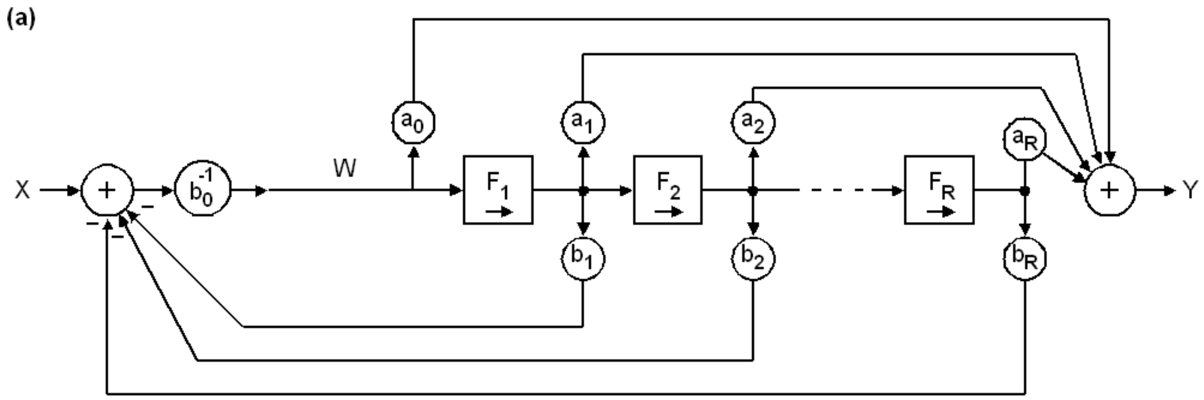

Fig. 3.2.1: **(a)** typical distributed feed-out topology. How can we open the loop to measure forward network F and (open) loop gain FB.

Understanding the network in Fig. 3.2.1(a) is difficult. To make it easier, we

- double the feed-forward elements $F_\#$ for #=1…R and use them in parallel, as illustrated in Fig. 3.2.1(b). The network is the same, because the nodes experience no feed-in,
- cut wire W, so that we get the new input wire L.

Measure the feed-forward network at open loop with $E = L = 0$:

$$F = \left.\frac{Y}{X}\right|_{L=0} = \frac{1}{b_0} \cdot \left[a_0 + a_1 F_1 + a_2 F_1 F_2 + ... + a_R (F_1 F_2 ... F_R)\right] \ . \tag{3.2.1}$$

To compute / measure the (open) loop-gain, feed a sinusoidal input signal to node L and measure it at node W, which delivers

$$FB = \left.\frac{W}{L}\right|_{X=0} = -\left[b_1 F_1 + b_2 F_1 F_2 + ... + b_R F_1 F_2 ... F_R\right] \frac{1}{b_0} \ . \tag{3.2.2}$$

The signal transfer function can then be computed as

$$STF = \frac{F}{1 - FB} = \frac{a_0 + a_1 F_1 + a_2 F_1 F_2 + ... + a_R F_1 F_2 \cdot ... \cdot F_R}{b_0 + b_1 F_1 + b_2 F_1 F_2 + ... + b_R F_1 F_2 \cdot ... \cdot F_R} \tag{3.2.3}$$

If we connect to W=L and compare Fig. parts (a) and (b), we will find that they operate identical.

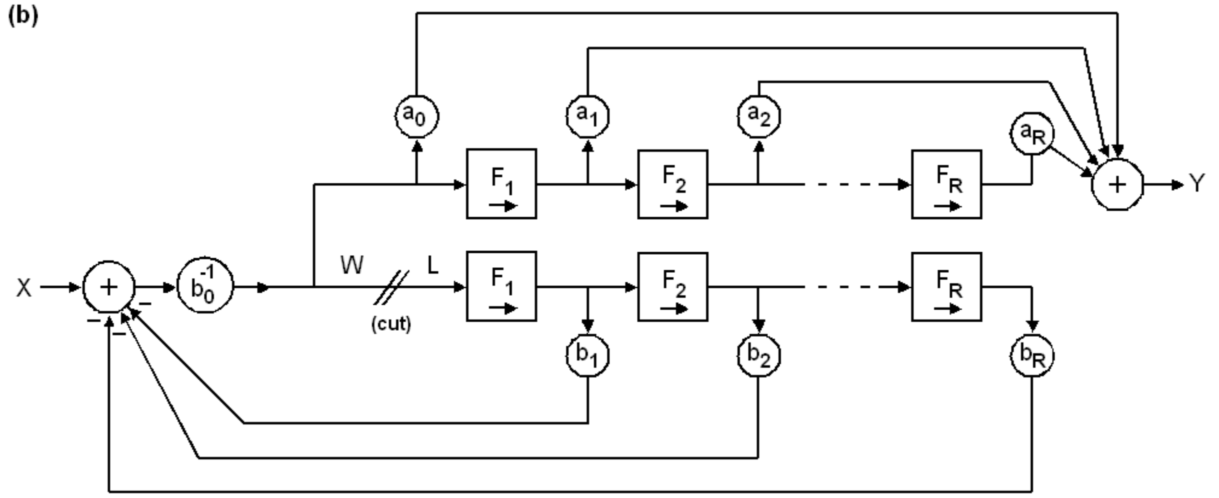

Fig. 3.2.1: (b) same network with 2 feed-forward paths and position of loop opening to measure forward network F and (open) loop gain FB.

3.3 Realizing Factor 1/b_0 in digital systems

Both topology 1 and 2 require continuous division by b_0. In digital systems, the division operator "/" is computed significantly slower than operators +, -, *.

In case of **real number** arithmetic

- we typically use scaled coefficients $a_\#^* = a_\# / b_0$ and $b_\#^* = b_\# / b_0$. This does not change the transfer functions but yields $b_0^* = 1$, avoiding the division.
- [In case $b_0 = 1$ is not possible, we should replace division by b_0 with a multiplication by *inv_b0*, computed as *inv_b0 = 1/b_0*, as multiplication computes faster than division.]

In case of **integer** or **bit-vector** arithmetic, $b_0 = 1$ is typically not possible. Example: $b_0 = 1$, $b_1 = 0.9734$, $b_2 = 0.0266$. Rounding to integers would deliver $b_1 = 1$ and $b_2 = 0$, which is inacceptable inaccurate. In this case, we do the following:

- Coefficients are typically computed as real numbers before conversion to integer.
- In their real number form, scale all coefficients to $a_\#^* = a_\# \cdot (2^M / b_0)$ and $b_\#^* = b_\# \cdot (2^M / b_0)$ with M being a positive Integer. This does not change the transfer functions but yields $b_0^* = 2^M$. Example: M=16, $b_0^* = 2^M = 65536$, $b_1^* = b_1 \cdot 2^M \cong round(0.9734 \cdot 2^M) = 63792$, $b_2^* = b_2 \cdot 2^M \cong round(0.0266 \cdot 2^M) = 1743$.
- As $b_0 = 2^M$, division by b_0 has to be performed, but can be realized as simple and fast M-bit shift-right operation.

4 Canonic Direct Structures

4.1 Time-Continuous Modeling

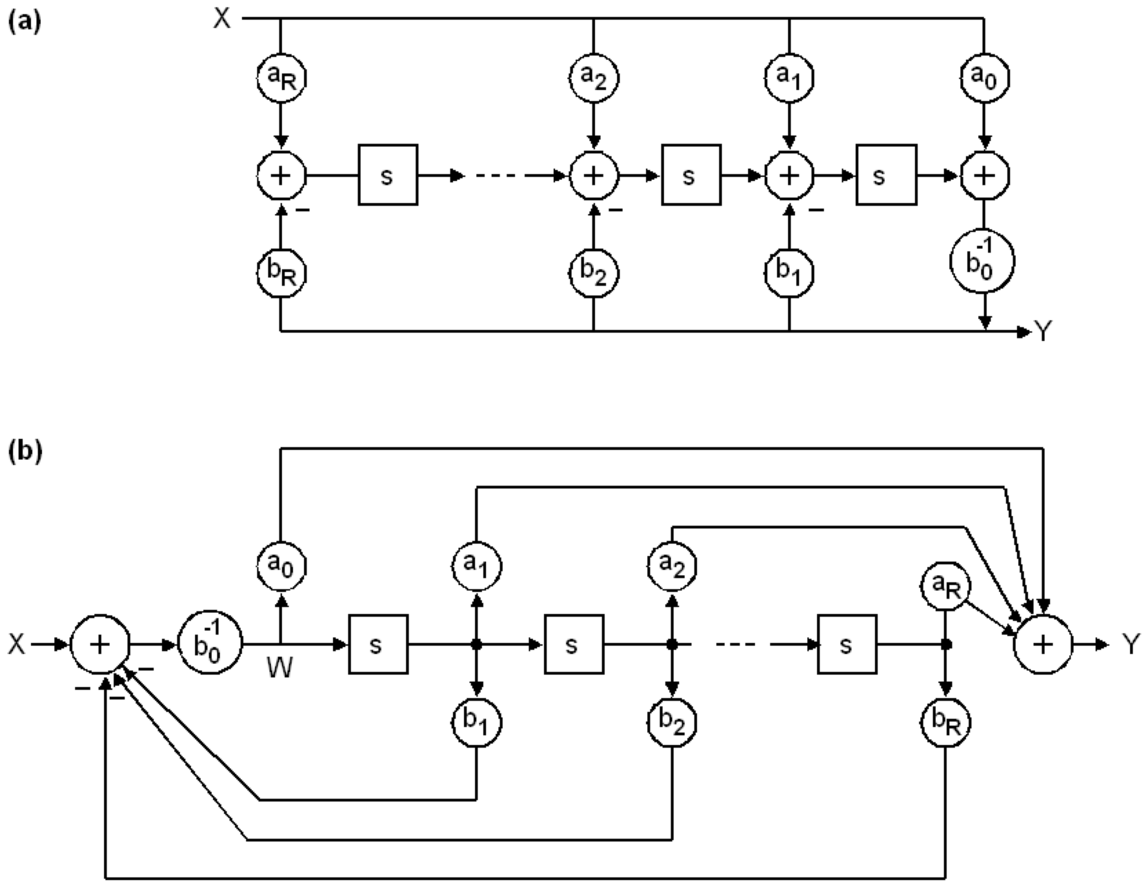

Fig. 4.1: Time-continuous filter of order *R* in (a) 1st and (b) second canonic direct structure. Typically, the boxes contain rather an integrator [s^{-1}] than a differentiator [s].

LTI models of time-continuous systems are modeled as

$$a_0 x(t) + a_1 \dot{x}(t) + ... + a_R x^{(R)}(t) = b_0 y(t) + b_1 \dot{y}(t) + ... + b_R y^{(R)}(t) \tag{4.1.1}$$

$$y(t) = b_0^{-1} \left[a_0 x(t) + a_1 \dot{x}(t) + ... + a_R x^{(R)}(t) - b_1 \dot{y}(t) - ... - b_R y^{(R)}(t) \right] \tag{4.1.2}$$

For frequency domain modeling we translate $x(t) \leftrightarrow X(s)$ and $\dot{x}(t) \leftrightarrow s \cdot X(s)$

$$a_0 X(s) + a_1 s X(s) + ... + a_R s^R X(s) = b_0 Y(s) + b_1 s Y(s) + ... + b_R s^R Y(s) \tag{4.1.3}$$

yielding transfer function $TF(s) = \dfrac{Y(s)}{X(s)} = \dfrac{a_0 + a_1 s + ... + a_R s^R}{b_0 + b_1 s + ... + b_R s^R}$ (4.1.4)

Using s=jω=j2π*f*: $TF(f=0) = a_0 / b_0$, $TF(f \to \infty) = a_R / b_R$ (4.1.5)

4.2 Time-Discrete Modeling

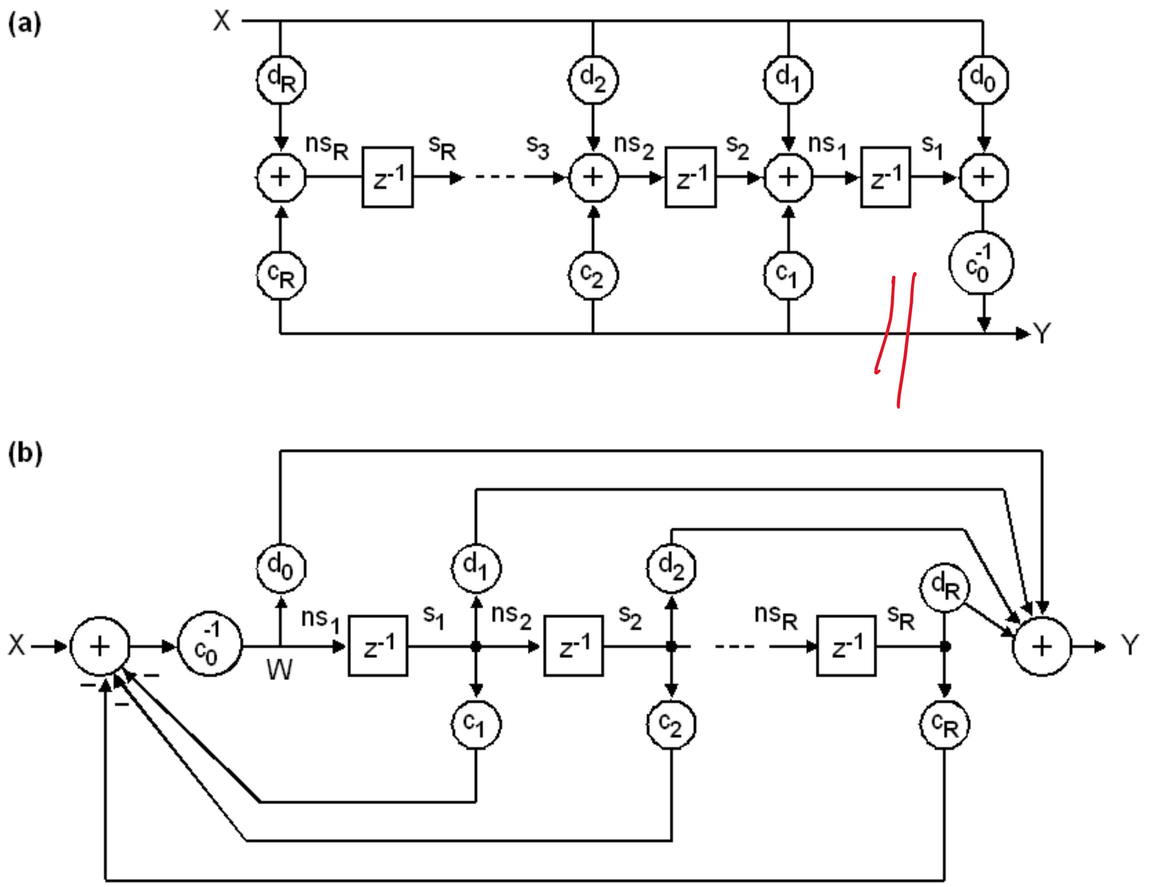

Fig. 4.2.1: Time-discrete filter of order R in (a) 1st and (b) 2nd canonic direct structure. How can we open the loops to measure forward network F and (open) loop gain FB?

Canonic: number of delays (z^{-1}) is R, with $z=exp(j2\pi F)$, with $F=f/f_s$ at sampling rate $f_s=1/T_s$. Direct structure: taps of impulse $h_n=h(n)$ response directly set by coefficients, whereas index n denotes time point $t_n = n\cdot T_s$.

$$d_0 x_n + d_1 x_{n-1} + \ldots + d_R x_{n-R} = c_0 y_n + c_1 y_{n-1} + \ldots + c_R y_{n-R} \quad \text{(scale to get } c_0 = 1 \text{ or } 2^M) \tag{4.2.1}$$

$$y_n = c_0^{-1}\left[d_0 x_n + d_1 x_{n-1} + \ldots + d_R x_{n-R} - c_1 y_{n-1} - \ldots - c_R y_{n-R}\right] \tag{4.1.2}$$

For frequency domain modeling we translate $x_n \leftrightarrow X(z)$ and $x_{n-k} \leftrightarrow z^{-k}\cdot X(z)$

$$c_0 Y(z) + c_1 z^{-1} Y(z) + c_2 z^{-2} Y(z) = d_0 X(z) + d_1 z^{-1} X(z) + d_2 z^{-2} X(z) \tag{4.1.3}$$

yielding transfer function $$TF(z) = \frac{d_0 + d_1 z^{-1} + \ldots + d_R z^{-R}}{c_0 + c_1 z^{-1} + \ldots + c_R z^{-R}} = \frac{d_0 z^R + d_1 z^{R-1} + \ldots + d_R}{c_0 z^R + c_1 z^{R-1} + \ldots + c_R} \tag{4.1.4}$$

$$TF(F=0) = TF(1) = \frac{d_0 + d_1 + \ldots + d_R}{c_0 + c_1 + \ldots + c_R}, \quad TF(F=0.5) = \frac{d_0 - d_1 + d_2 - d_3 \ldots}{c_0 - c_1 + c_2 - c_3 \ldots}, \quad h_0 = \frac{d_0}{c_0} \tag{4.1.5}$$

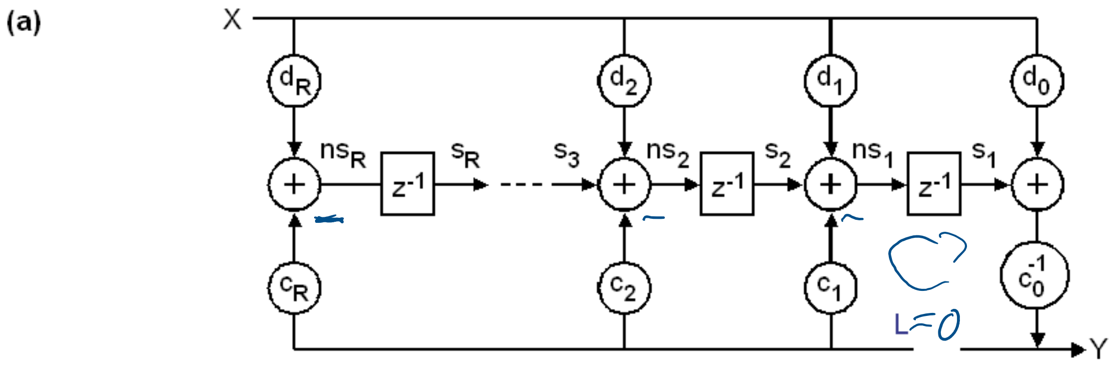

Fig. 4.2.2: Opening the loop of the filter in 1st canonic structure to measure forward network $F = Y/X$ @ $L=0$ and (open) loop gain $FB = Y/L$ @ $X=0$.

$$F = \frac{Y}{X}\Big|_{L=0} = c_0^{-1}\left[d_0 + d_1 z^{-1} + d_2 z^{-2} + \ldots + d_R z^{-R}\right.$$

$$FB = \frac{Y}{L}\Big|_{X=0} = -c_0^{-1}\left[c_1 z^{-1} + c_2 z^{-2} + \ldots + c_R z^{-R}\right]$$

$$STF = \frac{F}{1-FB} = \frac{\qquad}{c_0 + c_1 z^{-1} + c_2 z}$$

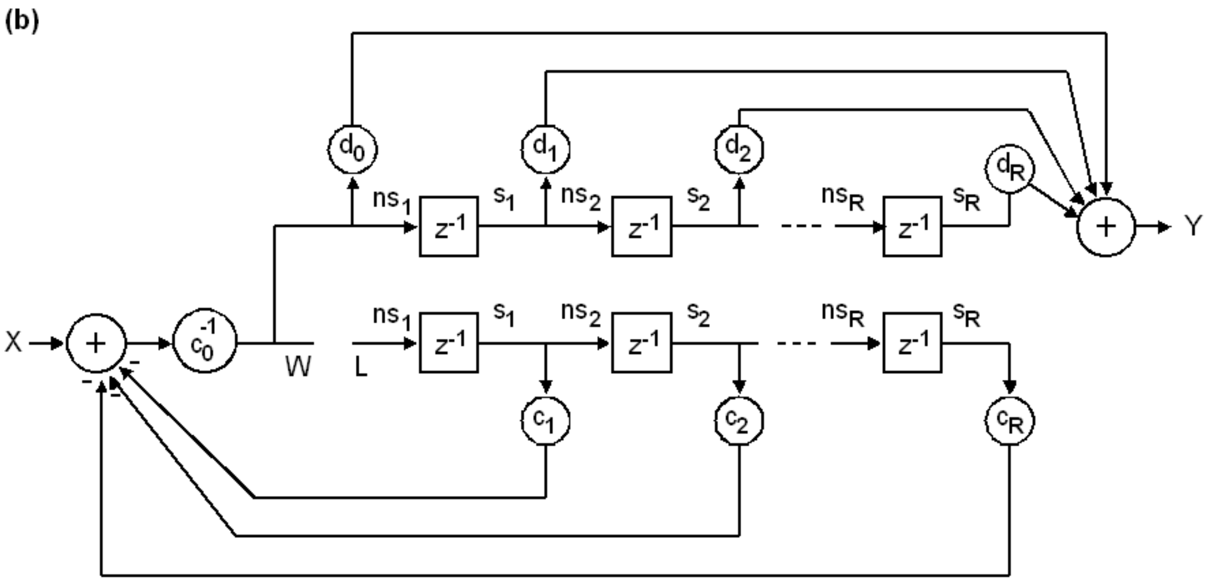

Fig. 4.2.3: Opening the loop of the filter in 2st canonic structure to measure forward network $F = Y/X$ @ $L=0$ and (open) loop gain $FB = W/L$ @ $X=0$.

5 Translating LTI Systems from s → z

The accurate relationship behaves difficult in formulae:

$z = e^{sT}$ ⇔ because sampling frequency $f_s = 1/T$. (5.0.1)

5.1 Linear Interpolation Using Backward / Forward Euler

Backward Euler: $\dot{x}(t) \cong \frac{x_n - x_{n-1}}{T}$ translates to $s \cdot X \cong \frac{X - z^{-1}X}{T} = \frac{1-z^{-1}}{T}X$. Cancelling X delivers

$$s \cong \frac{1-z^{-1}}{T} = f_s(1-z^{-1}) \quad \text{with} \quad f_s = 1/T. \tag{5.1.1}$$

Forward Euler: $\dot{x}(t) \cong \frac{x_{n+1} - x_n}{T}$ translates to $s \cdot X \cong \frac{z \cdot X - X}{T} = \frac{z-1}{T}X$. Cancelling X delivers

$$s \cong \frac{z-1}{T} = f_s(z-1). \tag{5.1.2}$$

Procedure to translate a 2nd order transfer function from *s* to *z* using backward Euler:

1. Scale the coefficients with sampling frequency f_s: $a_k^* = a_k \cdot f_s^{\,k}$, $b_k^* = b_k \cdot f_s^{\,k}$, k=0, 1, 2

2. Replace $s \rightarrow (1\text{-}z^{-1})$ and compute $H(z)$. Coefficients d_k^x, c_k^x:

$$d_0^x = a_0^* + a_1^* + a_2^* , \qquad d_1^x = -a_1^* - 2a_2^* , \qquad d_2^x = a_2^* \tag{5.1.3}$$

$$c_0^x = b_0^* + b_1^* + b_2^* , \qquad c_1^x = -b_1^* - 2b_2^* , \qquad c_2^x = b_2^* \tag{5.1.4}$$

This transfer function will already work well, but computationally inefficient as $c_0^x \neq 1$

$$H_s(s) = \frac{a_0 + a_1 s + a_2 s^2}{b_0 + b_1 s + b_2 s^2} \rightarrow H^x(z) = \frac{a_0^* + a_1^*\left(1-z^{-1}\right) + a_2^*\left(1-z^{-1}\right)^2}{b_0^* + b_1^*\left(1-z^{-1}\right) + b_2^*\left(1-z^{-1}\right)^2} = \frac{d_0^x + d_1^x z^{-1} + d_2^x z^{-2}}{c_0^x + c_1^x z^{-1} + c_2^x z^{-2}} \tag{5.1.5}$$

3. To obtain $c_0 = 1$ we divide all coefficients of $H(z)$ by coefficient c_0^x

$$d_k = d_k^x / c_0^x , \qquad c_k = c_k^x / c_0^x , \qquad k=0, 1, 2 \tag{5.1.6}$$

   yielding

$$H(z) = \frac{d_0^x + d_1^x z^{-1} + d_2^x z^{-2}}{c_0^x + c_1^x z^{-1} + c_2^x z^{-2}} = \frac{d_0 + d_1 z^{-1} + d_2 z^{-2}}{1 + c_1 z^{-1} + c_2 z^{-2}} \tag{5.1.7}$$

5.2 Bilinear (Tustin) Approximation

From series expansion of $ln(x)$ we approximate $$s=\frac{2}{T}\frac{1-z^{-1}}{1+z^{-1}}=2f_s\frac{1-z^{-1}}{1+z^{-1}} \tag{5.2.1}$$

Using $$\omega^*=\omega\frac{T}{2} \quad\Leftrightarrow\quad s^*=j\omega^*=s\frac{T}{2} \tag{5.2.2}$$

results in transformation $$s^*=\frac{1-z^{-1}}{1+z^{-1}} \quad\Leftrightarrow\quad z^{-1}=\frac{1-s^*}{1+s^*} \tag{5.2.3}$$

suffers from no amplitude error as $$\left|z^{-1}\right|=1=\left|\frac{1-j\omega^*}{1+j\omega^*}\right| \tag{5.2.4}$$

but frequency shift $$\omega_z^*=\arctan(\omega_s^*) \quad\Leftrightarrow\quad \omega_z=\frac{2}{T}\arctan\left(\omega_s\frac{T}{2}\right) \tag{5.2.5}$$

with ω_s being the original frequency axis of $H(s)$ and ω_z the compressed axis of $H(z)$. To get a particular frequency ω_x to the right point after translation to z, prewarp (German: vorverzerren) it according to

$$\omega_{s,prewarp}^*=\tan(\omega_s^*) \tag{5.2.6}$$

Procedure to translate a 2nd order transfer function from *s* to *z* using Tustin:

1. $a_k^*=a_k\cdot(2f_s)^k$, $b_k^*=b_k\cdot(2f_s)^k$, $k=0\ldots R$
2. Replace $s\rightarrow\frac{1-z^{-1}}{1+z^{-1}}$
3. Compute $H^x(z)$ with $c_0^x\neq 1$.
4. Divide all coefficients by c_0^x to obtain c_k, d_k with $c_0=1$.

Application for 2nd order:

$$H_s(s)=\frac{a_0+a_1s+a_2s^2}{b_0+b_1s+b_2s^2} \quad\rightarrow\quad H^x(z)=\frac{a_0^*+a_1^*\frac{1-z^{-1}}{1+z^{-1}}+a_2^*\left(\frac{1-z^{-1}}{1+z^{-1}}\right)^2}{b_0^*+b_1^*\frac{1-z^{-1}}{1+z^{-1}}+b_2^*\left(\frac{1-z^{-1}}{1+z^{-1}}\right)^2} \quad\rightarrow$$

$$H(z)=\frac{d_0+d_1z^{-1}+d_2z^{-2}}{1+c_1z^{-1}+c_2z^{-2}}$$

$a_k^*=a_k\cdot(2f_s)^k$, $b_k^*=b_k\cdot(2f_s)^k$, k=0, 1, 2

1st order system:		2nd order system		
$d_0^x=a_0^*+a_1^*$,	$d_1^x=a_0^*-a_1^*$	$d_0^x=a_0^*+a_1^*+a_2^*$,	$d_1^x=2a_0^*-2a_2^*$,	$d_2^x=a_0^*-a_1^*+a_2^*$
$c_0^x=b_0^*+b_1^*$,	$c_1^x=b_0^*-b_1^*$	$c_0^x=b_0^*+b_1^*+b_2^*$,	$c_1^x=2b_0^*-2b_2^*$,	$c_2^x=b_0^*-b_1^*+b_2^*$

$d_k=d_k^x/c_0^x$, $c_k=c_k^x/c_0^x$, k=0, 1, 2

5.3 Impulse-Invariant Time-Discretization

Basic principle:

1. Translate the analog frequency response $H_c(s)$ to a time-continuous impulse response $h_c(t)$.
2. Find a time-discrete model $H_d(z)$ that generates an impulse response $h_d(n)$, which samples $h_c(t)$, so that $h_d(n) = h_c(nT)$, where $T=1/f_s$ is the sampling interval.

Example:

A *RC* lowpass features the impulse response $h_c(t) = \begin{cases} 0 & if \quad t<0 \\ e^{-t/RC} & if \quad t \geq 0 \end{cases}$ shown in Fig. 4.4(b).

From Fig. 5.3(a) we derive $H_d(z) = \dfrac{a \cdot z^{-1}}{1-b \cdot z^{-1}} = \dfrac{a}{z-b}$. It is easily found by trial and error that its impulse response is 0, 1, b, b^2, b^3, b^4,... As illustrated in Fig. 4.4(b) the taps of $y(n)$ "sample" the impulse response of an *RC* lowpass (dashed lined) when $b = e^{-\omega_g T} = e^{-T/RC}$ and $a = 1-b$.

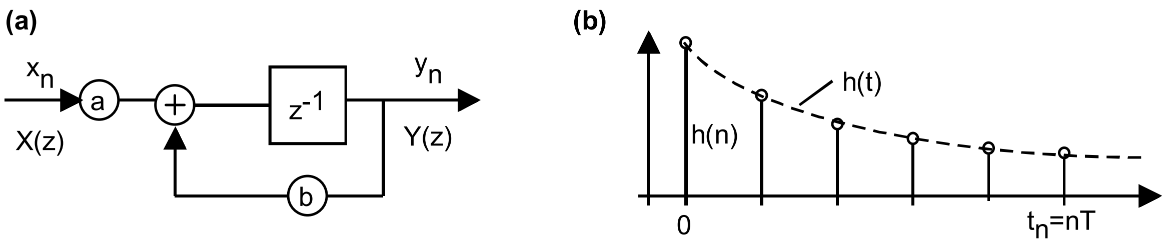

Fig. 5.3: (a) recursive IIR filter, **(b)** impulse response: time-discrete versus *RC* lowpass.

5.4 Matlab

Matlab's function *c2d* translates Matlab's time-continuous LTI systems to Matlab's time-discrete LTI systems. The conversion method can be selected. The reverse function is *d2c*.

6 Dealing with Poles and Zeros in Transfer Functions

This chapter should be unnecessary in this document. However, the author made the experience, that it is besser to explain it.

6.1 Pole im Orts- und Bode-Diagramm

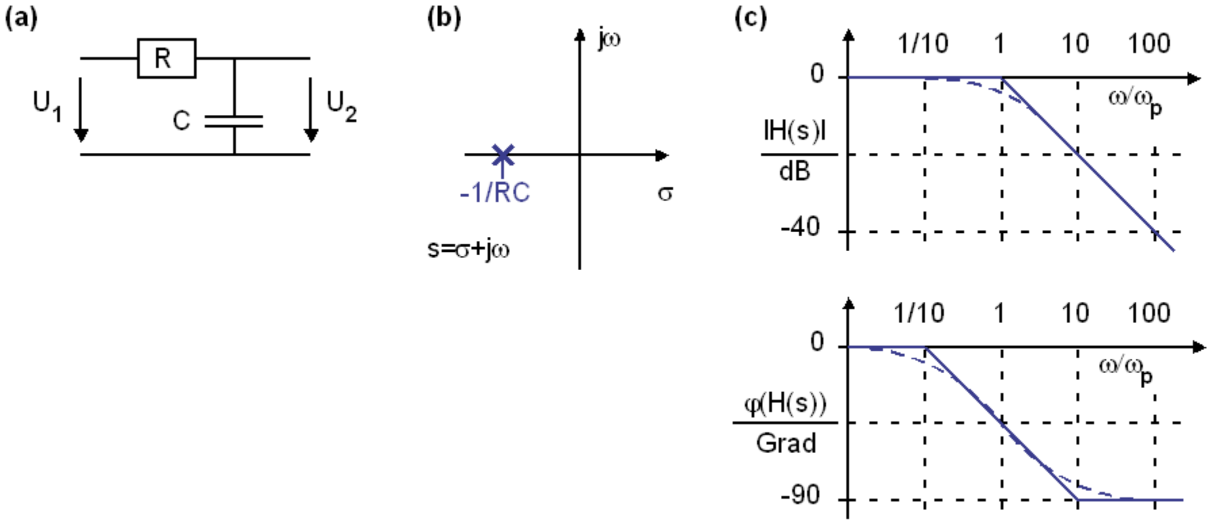

Fig. 6.1: (a) Schaltung mit Pol, **(b)** Lage des Pols in der komplexen *s*-Ebene, **(c)** Bode-Diagramm mit Betrag und Phase der Übertragungsfunktion. Gestrichelt: exakt, durchgezogen: Asymptotennäherung.

$$H(s) = \frac{1/sC}{R + 1/sC} = \frac{1}{1 + sRC} = \frac{1}{1 - s/(-1/RC)} = \frac{1}{1 - s/s_p} \qquad => \qquad s_p = -1/RC\,.$$

Bild 1.6.1 zeigt ein System mit einem Pol, gelegen in $s_p = 1/RC$ in der komplexen *s*-Ebene. Ein System ist stabil, wenn alle seine Pole in der negativen halbebene liegen. Alle Reaktionen am Ausgang klingen ab, wenn der Eingang Null ist.

Pol (in linker *s*-Halbebene) → „alles unten“: Nullstelle im Nenner (unter dem Bruchstrich), Knick nach unten im Amplitudendiagramm, Stufe um -90° nach unten im Phasendiagramm. Ein Pol in der linken *s*-Halbebene bewirkt im Amplitudengang einen Knick nach „unten“, und zwar in der Polfrequenz $\omega_p=|s_p|$, wenn man in Richtung $f\to\infty$ schaut. Die Asymptoten von $|H(s)|$ haben einen Schnittpunkt im Pol. Bei Leistungen beträgt der Knick im Pol -10dB/dec, bei Spannungen und Strömen -20dB/dec. Im Pol beobachten wir eine Phasendrehung von genau -45°, die Phasendrehung beginnt bei ca. $\omega_p/10$ und endet mit -90° bei ca. 10 ω_p.

Amplitudenfehler der Tangentennäherung in ω/ω_p=1: 3 dB
Phasenfehler der Tangentennäherung in ω/ω_p=1: 0°
Phasenfehler der Tangentennäherung in ω/ω_p=0,1: arctan(0,1) = 5,71°
Phasenfehler der Tangentennäherung in ω/ω_p=10: arctan(10) – 90° = -5,71°

Frage: Was bewirkt eine Polstelle in der rechten Laplace-Halbebene (Realteil <0)?
Lösung: Polstelle in positiver Halbebene: Instabilität da aufklingende Schwingung. Das System verhält sich ohne Anregung gemäß $\exp(s_p \cdot t)$, also aufklingend, wenn $s_p > 0$, abklingend wenn $s_p < 0$.

6.2 Nullstellen im Orts- und Bode-Diagramm

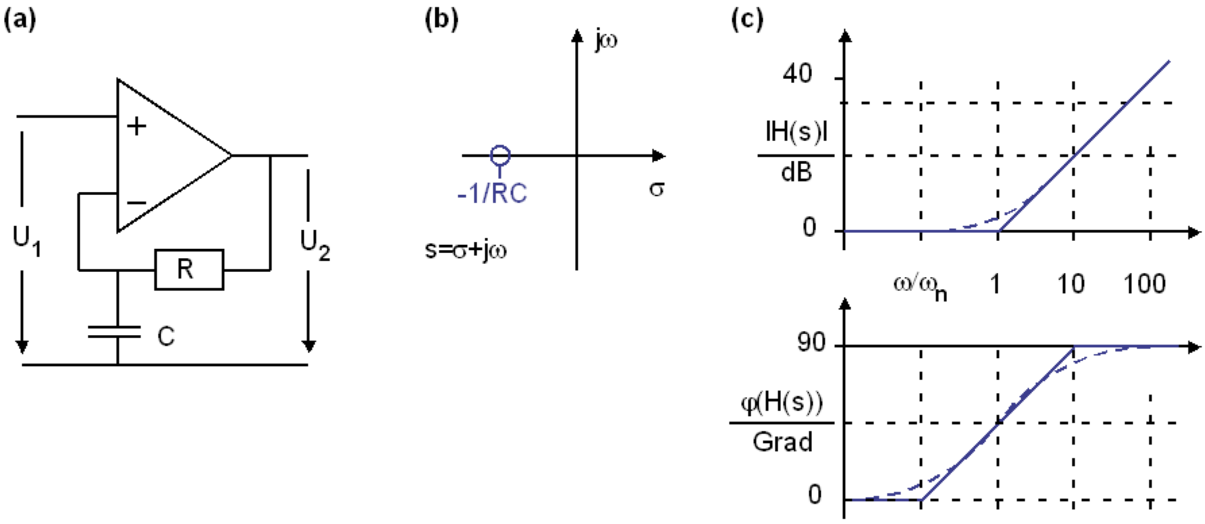

Fig. 6.2: Das Verhalten des Tiefpasses wird im Rückkopplungsnetzwerk eines Operationsverstärkers invertiert: **(a)** Schaltung mit Nullstelle, **(b)** Lage der Nullstelle in der komplexen *s*-Ebene, **(c)** Bode-Diagramm mit Betrag und Phase der Übertragungsfunktion. Gestrichelt: exakt, durchgezogen: Asymptotennäherung.

$$H(s) = \left[\frac{1}{1+sRC}\right]^{-1} = 1+sRC = 1-s/(-1/RC) = 1-s/s_n \quad => \quad s_n = -1/RC\,.$$

Fig. 6.1.2 zeigt ein System mit einer Nullstelle, gelegen in $s_n = 1/RC$ in der komplexen *s*-Ebene, da die OP-Schaltung das Verhalten des Rückkopplungsnetzwerkes invertiert.

Nullstelle (in linker *s*-Halbebene) → „alles oben“: Nullstelle im Zähler (über Bruchstrich), Knick nach oben im Amplitudendiagramm, Stufe um +90° nach oben im Phasendiagramm. Eine Nullstelle in der linken *s*-Halbebene bewirkt im Amplitudengang einen Knick nach „oben“, und zwar in der Nullstellenfrequenz $\omega_p=|s_p|$, wenn man in Richtung $f\to\infty$ schaut. Die Asymptoten von $|H(s)|$ haben einen Schnittpunkt in der Nullstelle. Bei Leistungen beträgt der Knick +10dB/dec, bei Spannungen und Strömen +20dB/dec. In der Nullstelle beobachten wir eine Phasendrehung von +45°, sie beginnt bei ca. $\omega_n/10$ und endet mit +90° bei ca. 10 ω_n.

Amplitudenfehler der Tangentennäherung in ω/ω_n=1: -3 dB
Phasenfehler der Tangentennäherung in ω/ω_n=1: 0°
Phasenfehler der Tangentennäherung in ω/ω_n=0,1: arctan(0,1) = -5,71°
Phasenfehler der Tangentennäherung in ω/ω_n=10: arctan(10) +90° = +5,71°

Frage: Was bewirkt eine Nullstelle in der rechten Laplace-Halbebene (Realteil <0) ?

Lösung: Nullstellen in der rechten s-Halbebene verhalten sich im Amplitudendiagramm wie Nullstellen in der negativen Halbebene, drehen aber die Phase umgekehrt, also nach unten. Während Nullstellen in der linken *s*-Halbebene in der Regelungstechnik zum Gewinn von Phasenreserve dienen, kosten sie in der rechten Halbebene Phasenreserve → vergrößerte Instabilität.

6.3 Faktorisieren v. Übertragungsfunkt. in Pole u. Nullstellen

Ein Polynom der Ordnung N lässt sich in seine N Nullstellen $s_{p\#}$ mit #=1...N, faktorisieren:

$$s^N + \ldots + b_3 s^3 + b_2 s^2 + b_1 s + b_0 = (s - s_{p1}) \cdot (s - s_{p2}) \cdot \ldots \cdot (s - s_{pN})$$

Sind die Koeffizienten $b_0, b_1, \ldots b_N$ reell, dann sind die Nullstellen entweder reell oder konjugiert komplexe Paare $s_{p1,2} = \sigma_p \pm j\omega_p$. Ein solches Nullstellenpaar lässt sich in ein Polynom zweiter Ordnung mit reellen Koeffizienten zusammenfassen. Mit $s_{p1} = \sigma_p + j\omega_p$ und $s_{p1} = \sigma_p - j\omega_p$ ergibt sich

$$(s - s_{p1}) \cdot (s - s_{p2}) = s^2 - 2\sigma_p + (\sigma_p^2 + \omega_p^2),$$

was für Polpaare mit $\omega_0^2 = \sigma_p^2 + \omega_p^2$ oft in der Form

$$(s - s_{p1}) \cdot (s - s_{p2}) = s^2 + 2D\omega_0 s + \omega_0^2$$

dargestellt wird. Daraus lässt sich das Poolpaar mit

$$s_{p1,2} = \sigma_p \pm j\omega_p = -\omega_0 \left(D \pm j\sqrt{1 - D^2} \right)$$

zurückgewinnen. Daraus ist ersichtlich, dass bei komplexen Poolpaaren $|s_{p1,2}| = \omega_0$. Die Dämpfungskonstante D beschreibt die Dämpfung von pro Schwingung und Grenzfrequenz ω_0 die Knickfrequenz, ab welcher das Amplitudendiagramm um -40dB/dec nach unten abknickt, und in welcher eine Phasendrehung von -90° verursacht wird.

Jede Übertragungsfunktion in s lässt sich also faktorisieren in ihre Pole und Nullstellen:

$$H(s) = \frac{Y(s)}{X(s)} = K \frac{s^M + \ldots + a_2 s^2 + a_1 s + a_0}{s^N + \ldots + b_2 s^2 + b_1 s + b_0} = K \frac{(s - s_{n1}) \cdot (s - s_{n2}) \cdot \ldots \cdot (s - s_{nM})}{(s - s_{p1}) \cdot (s - s_{p2}) \cdot \ldots \cdot (s - s_{pN})}$$

mit K konstant, X(s), $Y(s)$ Laplace-Transformierte der Ein- und Ausgangssignale $x(t)$, $y(t)$.

Anzahl Nullstellen: M Anzahl Pole: N

Ordnung Zählerpolynom: M Ordnung Nennerpolynom: N

Ordnung der Übertragungsfunktion $H(s)$: Maximum von M und N

Nullstellen von H(s): $s_{n1}, s_{n2}, \ldots, s_{nM}$ Pole von H(s): $s_{p1}, s_{p2}, \ldots, s_{pN}$

Ein natürliches System verhält sich bei hinreichend hohen Frequenzen immer träge, so dass letztendlich in der Natur immer $N > M$ sein muss.

6.4 Konjugiert-komplexes Nullstellen-Paar auf der $j\omega$-Achse

Konjugiert-komplexe Nullstellenpaare auf der $j\omega$-Achse markieren ein sogenanntes Notch-Filter, (engl. notch = Kerbe), welches eine bestimmte Frequenz mit einer schmalen Kerbe ("notch") im Bode-Diagramm unterdrückt. Solche Filter werden beispielsweise zur Unterdrückung von Rückkopplungen (Pfeifton) angewendet.

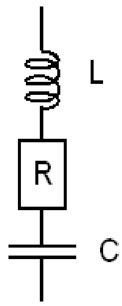

Fig. 6.4: Serien-Schwingkreis

Beispiel: Ein RLC-Serienschwingkreis hat die Impedanz

$$Z_{ser}(s) = \frac{1}{sC} + R + sL = \frac{1 + RC\cdot s + LC\cdot s^2}{sC} = \frac{L}{s}\left(\frac{1}{LC} + \frac{R}{L}s + s^2\right) \tag{1.6.4.1}$$

mit den Polen $s_{n1,2} = \frac{R}{2L} \pm j\sqrt{\frac{1}{LC} - \left(\frac{R}{2L}\right)^2} \xrightarrow{R\to 0} \pm j\sqrt{\frac{1}{LC}} = \pm j\omega_0$. (1.6.4.2)

Mit $s = j\omega$ erhält man $Z_{ser}(s = j\omega) = \frac{(1-\omega^2/\omega_0^2) + j\omega RC}{j\omega C}$. In der Resonanzfrequenz $\omega_0 = 1/\sqrt{LC}$ beträgt die Übertragungsfunktion $Z_{ser}(\omega_0) = R$, so dass für sehr $R \to 0$ die gesamte Impedanz gegen $Z_{ser}(\omega_0) = \xrightarrow{R\to 0} 0$ geht und die Nullstellen gemäß Gl. (1.6.4.2) bei $\pm j\omega_0$ auf der $j\omega$-Achse liegen.

6.5 Konjugiert-komplexes Polpaar auf der *jω*-Achse

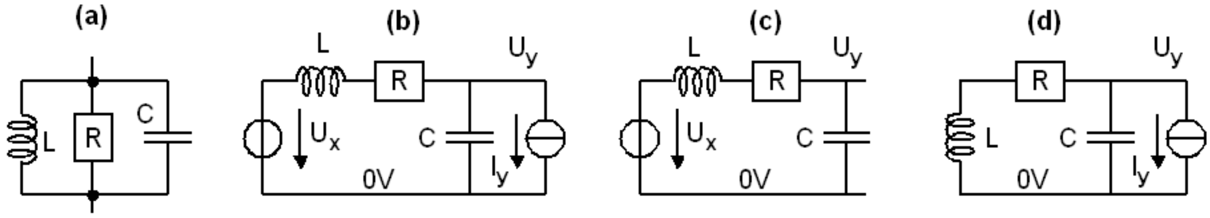

Fig. 6.5: (a) RLC–Parallelschwingkreis, **(b)** RLC-Tiefpass mit Eingangsspannung U_x und Laststrom I_y, **(c)** Spezialfall $I_y = 0$ in Bildteil (b) und **(d)** Spezialfall $U_x = 0$ in Bildteil (b).

Konjugiert-komplexe Polpaare auf der *jω*-Achse markieren einen Oszillator.
Beispiel: Ein RLC-Parallelschwingkreis hat die Impedanz

$$Z_{par}(s) = \frac{1}{sC} \| R \| sL = \frac{L \cdot s}{1 + (L/R) \cdot s + LC \cdot s^2} \tag{1.6.5.1}$$

mit den Polen $s_{p1,2} = \frac{1}{2RC} \pm j\sqrt{\frac{1}{LC} - \left(\frac{1}{2RC}\right)^2} \xrightarrow{R\to\infty} \pm j\sqrt{\frac{1}{LC}} = \pm j\omega_0$. (1.6.5.2)

Mit s = jω erhält man $Z_{ser}(s = j\omega) = \frac{j\omega L}{(1-\omega^2/\omega_0^2) + j\omega L/R}$. In der Resonanzfrequenz $\omega_0 = 1/\sqrt{LC}$ beträgt die Übertragungsfunktion $Z_{par}(\omega_0) = R$, so dass für sehr $R \to \infty$ die gesamte Impedanz gegen $Z_{par}(\omega_0) = \xrightarrow{R\to\infty} \infty$ geht und die Pole gemäß Gl. (1.6.4.4) bei $\pm j\omega_0$ auf der *jω*-Achse liegen. Nach Abschalten der Anregung (*x*=0) könnte daher ein angeregter, verlustfreier Schwingkreis unendlich lange weiterschwingen.

Die Übertragungsfunktion des RLC-Tiefpasses in Bildteil (b) ergibt sich aus (c) und (d) zu

$$PTF(s) = \left.\frac{U_y}{U_x}\right|_{I_y=0} = \frac{1/sC}{(1/sC) + (R + sL)} = \frac{1}{1 + RC \cdot s + LC \cdot s^2} \tag{1.6.5.3}$$

$$-QTF(s) = \left.\frac{U_y}{-I_y}\right|_{U_x=0} = (1/sC) \| (R + sL) = \frac{R + sL}{1 + RC \cdot s + LC \cdot s^2} \tag{1.6.5.4}$$

mit den Polen $s_{p1,2} = \frac{R}{2L} \pm j\sqrt{\frac{1}{LC} - \left(\frac{R}{2L}\right)^2} \xrightarrow{R\to 0} \pm j\sqrt{\frac{1}{LC}} = \pm j\omega_0$. (1.6.5.5)

In der Resonanzfrequenz strebt die Ausgangsspannung $U_y \xrightarrow{R\to 0} \infty$.

6.6 Inversion der Übertragungsfunktion

Sei $Y(s) = H(s)\, X(s)$. Gesucht ist die Umkehrfunktion $G(s)$, so dass $X(s) = G(s)\, Y(s)$:

$$G(s) = \frac{1}{H(s)} = \frac{1}{K} \frac{(s-s_{p1})\cdot(s-s_{p2})\cdot\ldots\cdot(s-s_{pN})}{(s-s_{n1})\cdot(s-s_{n2})\cdot\ldots\cdot(s-s_{nM})}$$

Die inverse Übertragungsfunktion $G(s) = H^{-1}(s)$ erhält man im Bode-Diagramm durch Spiegelung von $H(s)$ an der 0dB-Achse.

Folgerungen:

Wo $H(s)$ eine Nullstelle hat, da hat $G(s)$	einen Pol
Wo $H(s)$ einen Pol hat, da hat $G(s)$	eine Nullstelle
Beschreibt $H(s)$ einen Tiefpass, dann beschreibt $G(s)$	einen Hochpass
Beschreibt $H(s)$ einen Hochpass, dann beschreibt $G(s)$	einen Tiefpass
Beschreibt $H(s)$ einen Bandpass, dann beschreibt $G(s)$	eine Bandsperre
Beschreibt $H(s)$ eine Bandsperre, dann beschreibt $G(s)$	einen Bandpass

Rückgekoppelte Systeme (z.B. Operationsverstärker) verhalten sich bei hinreichend hoher Schleifenverstärkung gemäß ihrer sogenannten Signaltransferfunktion $STF(s) \cong 1/B(s)$, wobei $B(s)$ die Übertragungsfunktion des Rückkopplungsnetzwerks ist, $F(s)$ die Übertragungsfunktion des Vorwärtsnetzwerks und $FB(s) = F(s)\cdot B(s)$ die Schleifenverstärkung. [Notation im Bild: $A^* = STF,\ k = B$.] Folgerung: Ist das Rückkopplungsnetzwerk ein Hochpass, dann verhält sich das Gesamtsystem als Tiefpass und umgekehrt.

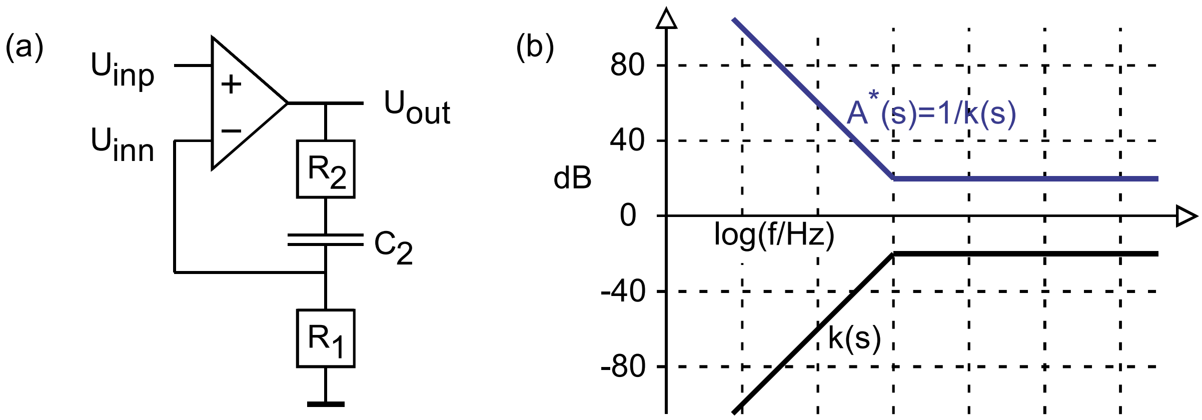

Fig. 6.6: (a) Operationsverstärker mit Rückkopplungsnetzwerk, **(b)** Übertragungsfunktion des Rückkopplungsnetzwerks $B(s)$ und der Gesamtschaltung: $STF(s) \cong 1/B(s)$.: Die Übertragungsfunktion von B wird invertiert. [Notation im Bild: $A^* = STF,\ k = B$.]

7 System Stability

7.1 The Impact of Poles and Zeros on Loop Stability

7.1.1 General

Computing poles (i.e. zeros of the denominator) and zeros (of the numerator) of *STF* and *NTF* is often complicated and requires computer-aided tools. If we have these poles and zeros, we have deep system insight. Zeros describe the stimulation (dt. Anregung) and poles the momentum (dt. Eigendynamik) of a system.

$$STF = \frac{Y}{X} = \frac{F}{1+FB} \quad \Leftrightarrow \quad Y(1+FB) = FX \tag{7.1.1}$$

For X=0, both *STF* and *NTF* deliver

$$Y\cdot(1+FB) = 0 \tag{7.1.2}$$

If $Y \neq 0$, this equation is fulfilled if – and only if – s takes values (poles) s_p that fulfil the condition

$$1+FB(s_{p\#}) = 0 \quad \Leftrightarrow \quad FB(s_{p\#}) = -1. \tag{7.1.3}$$

An R^{th} order system has R poles $s_{p\#}$. In time-domain, this corresponds to output signal $y(t)$:

time-continuous: $$y(t) = \sum_k C_k e^{s_{p_k} t} \tag{7.1.4}$$

time-discrete: $$y_n = \sum_k C_k e^{s_p nT} = \sum_k C_k z_{p_k}^n \tag{7.1.5}$$

With C_k being constants and index $p_\#$ indicating pole number k. Fig. 5.2 illustrates the relation between the location of poles $s_p=\sigma_p+j\omega_p$ in the Laplace domain $s=\sigma+j\omega$ and the respective transient behavior. For a polynomial with real coefficients complex poles will always come as complex pairs $s_p=\sigma_p\pm j\omega_p$ that can be combined to $e^{\sigma_p t}\cos(\omega_p t)$ or $e^{\sigma_p t}\sin(\omega_p t)$, because $e^{jx}+e^{-jx} = 2\cdot\cos(x)$ and $e^{jx}-e^{-jx}=2j\cdot\sin(x)$. It is obvious that these functions increase with $\sigma_p>0$ and decay with negative $\sigma_p<0$.

The conclusion from a time-continuous to time-discrete is obvious from $z=e^{sT}$ and $e^{s_p T}$ with $T=1/f_s$ being the sampling interval. Increasing time corresponds to increasing n for z_p^n. Consequently, stability requires $\sigma_p<0$ or $|z_p|<1$ for all poles $s_{p,i}$ or $z_{p,1}$, respectively.

7.1.2 Second Order Lowpass

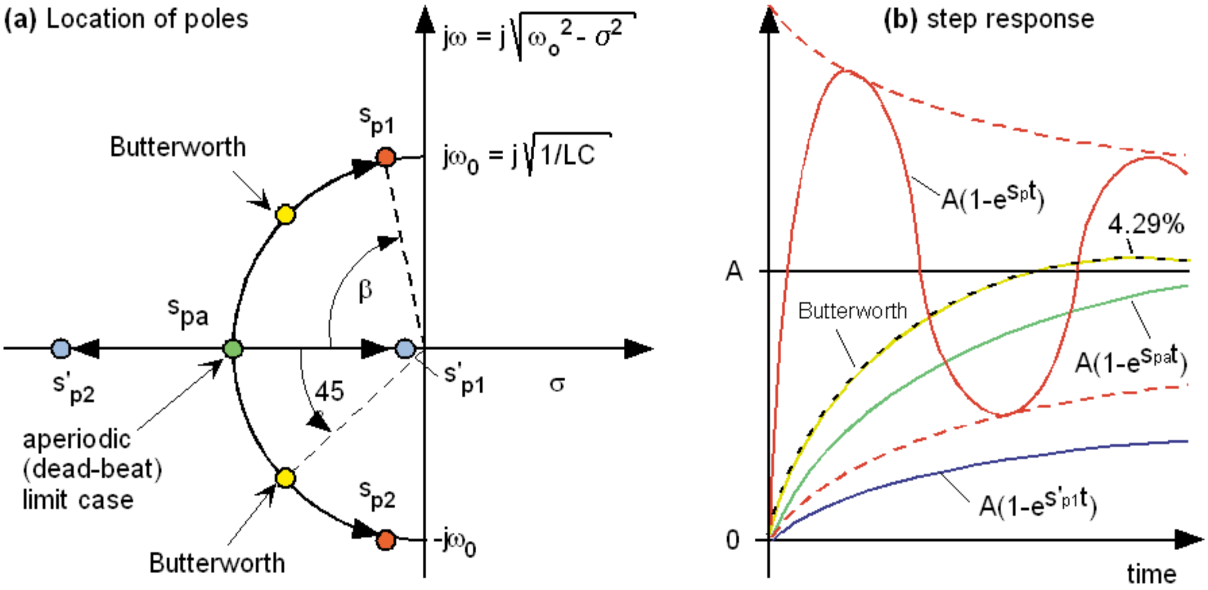

Fig. 7.1.2:. Time-continuous 2nd order lowpass: **(a)** poles, **(b)** time-domain step responses

A technically particularly important system is the 2nd order lowpass, frequently modeled as

$$H_{LP}(s) = \frac{A_0}{S^2 + 2DS + 1} = \frac{A_0\omega_0^2}{s^2 + 2D\omega_0 s + \omega_0^2} \tag{7.1.6}$$

with A_0 being the DC amplification, D damping (per wave) parameter, ω_0 bandwidth and $S = s/\omega_0$. Being relative to ω_0.

$$S_{p1,2} = -D\left(1 \pm \sqrt{1 - \frac{1}{D^2}}\right) = -D\left(1 \mp j\sqrt{\frac{1}{D^2} - 1}\right) \tag{7.1.7}$$

$$s_{p1,2} = -D\omega_0\left(1 \pm \sqrt{1 - \frac{1}{D^2}}\right) = -D\omega_0\left(1 \mp j\sqrt{\frac{1}{D^2} - 1}\right) \tag{7.1.8}$$

The *Butterworth* characteristics is typically regarded as optimal choice between speed (measured as settling time) and stability, which is identified by 4.29% step response voltage overshoot in time-domain.

In frequency domain, the *Butterworth* characteristics has neither ripple nor peaking and an amplitude drop of $1/\sqrt{2}$ corresponding to -3.01 dB at ω_0.

7.1.3 Characteristic Lowpasses

The *Butterworth* lowpass is the mathematically flattest characteristics in frequency domain and has always $1/\sqrt{2}$ corresponding to –3.01 dB attenuation in its cut-off frequency, regardless of its order. Its signal transfer is

$$\left|STF_{BW}(s)\right| = \frac{1}{\sqrt{1+\left|\frac{s}{\omega_0}\right|^{2N}}} \xrightarrow{s=j\omega} \frac{1}{\sqrt{1+\left|\frac{\omega}{\omega_0}\right|^{2N}}} \quad \Leftrightarrow \quad \left|H_{BW}(f)\right| = \frac{1}{\sqrt{1+\left|\frac{f}{f_0}\right|^{2N}}} \tag{7.1.9}$$

Note that this is a behavioral model obtaining an amplification of $1/\sqrt{2}$ at $f=f_0$.

Table 7.1.3: Poles for Butterworth (BW) lowpasses of 1st, 2nd, 3rd order, furthermore 45°-phase-margin (PM45) technique and aperiodic borderline case (AP). *Butterworth* coefficients for order N=1,2,3 taken from [https://de.wikipedia.org/wiki/Butterworth-Filter].

Lowpass Type	Denominator Poly. with $S=s/\omega_0$	D	Poles, represented as $\sigma_p \pm j\omega_p$	Φ_p, $\omega_p e^{\pm j\Phi_p}$	step resp. overshoot
AP1=BW1	$S+1$	-	$S_p = 1 \Leftrightarrow s_p = \omega_0$	0°	0%
AP2	$S^2+2S+1 = (S+1)^2$	1	$S_{p1,2} = 1 \Leftrightarrow s_{p1,2} = \omega_0$	0°	0%
BW2	$S^2 + \sqrt{2}\,S + 1$	$\sqrt{1/2}$	$S_{p1,2} = \sqrt{1/2}\cdot(1 \pm j)$	±45°	4%
BW3	$(S^2 + S + 1)\,(S+1)$	-	$S_{p1,2}=\frac{1}{2}\,(1+j\sqrt{3})$, $S_{p3}=1$	±60°, 0°	8%
PM45	$S^2 + S + 1$	1/2	$S_{p1,2} = \frac{1}{2}\,(1 + j\sqrt{3})$	±60°	16%

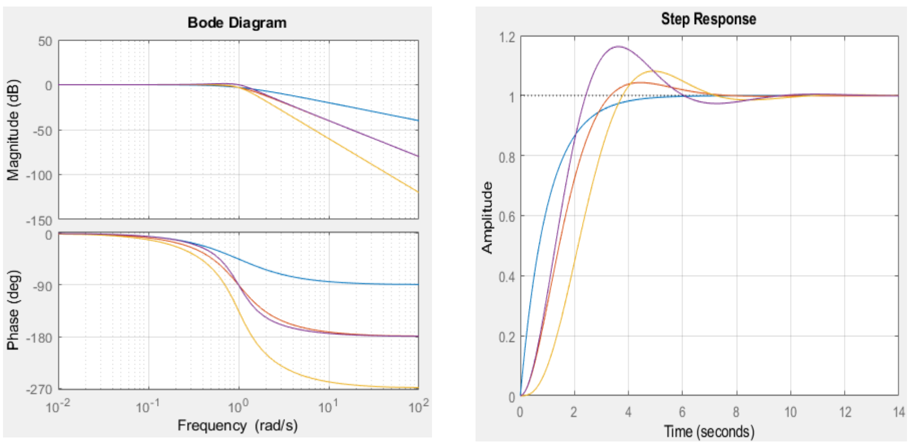

(a) Bode diagram (b) Step responses

Fig. 7.1.3: Characteristics of some lowpasses: Butterworth 1st order (blue), 2nd order (red), 3rd order (yellow) ϕ_M=45 (pink).

Listing 7.1.3: Matlab code for Fig. 7.1

```
% Filter: 2 poles
Hs_BW1=tf([1],[1 1]); Hs_BW2=tf([1],[1 sqrt(2) 1])
Hs_BW3=tf([1],[1 2 2 1]); Hs_M45=tf([1],[1 1 1])
figure(1); step(Hs_BW1,Hs_BW2,Hs_BW3,Hs_M45); grid on;
figure(2); h=bodeplot(Hs_BW1,Hs_BW2,Hs_BW3,Hs_M45); grid on;
%setoptions(h,'FreqUnits','Hz','PhaseVisible','on');
```

7.1.4 Example: 2nd Order (RLC) Lowpass

An RLC lowpass according to Fig. 7.1.4 is modeled as

$$H_{LP}(s) = \frac{1}{1 + RC \cdot s + LC \cdot s^2} \tag{7.1.10}$$

R is a sum of both voltage-source output impedance and inductor's copper resistor. Combining (7.1.6) yields $A_0 = 1$, $f_0 = \frac{1}{2\pi\sqrt{LC}}$ and $D = \frac{R}{2}\sqrt{\frac{C}{L}}$.

(a) RLC lowpass (b) Bode diagram (c) Step responses

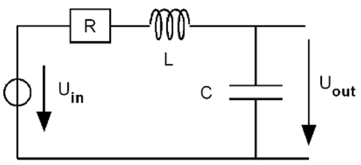

OSC: D=0.1: oscillating case
M45: D=½: phase marg. 45°
BW2: D=$\sqrt{1/2}$: Butterworth
AP2: D=1: aperiodic borderline

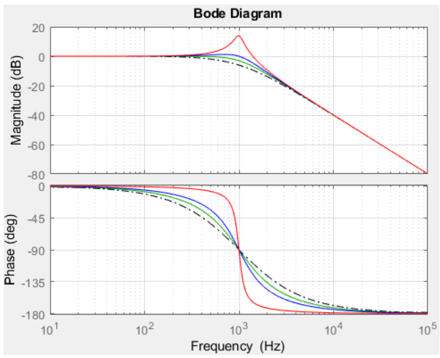

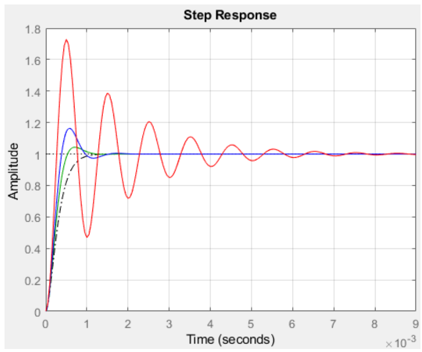

Fig. 7.1.4: Characteristics of an RLC lowpass.

Listing 7.1.4: Matlab code generating screen shots of Fig. 7.1.4 (b) and (c).

```
% RLC lowpass as filter with 2 poles
% ----------------------------------
% setting cut-off frequency f0 and restor R:
f0     = 10000; % set cut-off frequency in Hz
R      = 1;     % set resistor in Ohms
% Stability settings:
D_OSC = 0.1       ;  % 2nd order oscillating
D_BW2 = sqrt(1/2);   % Butterworth 2nd order
D_M45 = 1/2       ;  % phase margin 45°, 2n order
D_AP2 = 1.0001    ;  % aperiodic borderline case, 2nd order
% conclusions:
w0 = 2*pi*f0; LC = 1/w0^2;
L_OSC = R/(2*D_OSC*w0); C_OSC = 2*D_OSC/(R*w0);
L_M45 = R/(2*D_M45*w0); C_M45 = 2*D_M45/(R*w0);
L_BW2 = R/(2*D_BW2*w0); C_BW2 = 2*D_BW2/(R*w0);
L_AP2 = R/(2*D_AP2*w0); C_AP2 = 2*D_AP2/(R*w0);
% set up LTI systems:
Hs_AP2=tf([1],[LC R*C_AP2 1]);  % aperiodic borderline case, 2nd order
Hs_BW2=tf([1],[LC R*C_BW2 1]);  % Butterworth 2nd order
Hs_M45=tf([1],[LC R*C_M45 1]);  % phase margin 45°, 2n order
Hs_OSC=tf([1],[LC R*C_OSC 1]);  % 2nd order oscillating
% Graphical postprocessing
figure(1); step(Hs_AP2,'k-.',Hs_BW2,'g',Hs_M45,'b',Hs_OSC,'r'); grid on;
figure(2); h=bodeplot(Hs_AP2,'k-.',Hs_BW2,'g',Hs_M45,'b',Hs_OSC,'r');
grid on; p = bodeoptions; setoptions(h,'FreqUnits','Hz');
```

7.2 The Impact of Phase Margin on Loop Stability

7.2.1 How to Measure Phase Margin

Poles $s_{p\#}$ fulfilling the requirement $1+FB(s_{p\#}) = 0$ of Eq. (7.1.3) may be difficult to compute, particularly, when the order of the system is >2. There is an easier way to make a first stability estimation, because $1+FB = 0$ translates to

$$FB = -1, \tag{7.2.1}$$

which corresponds to

$$|FB| = 1 \text{ and } angle(FB) = -180° \text{ which is equivalent to } FB = 1 \cdot e^{-180°} \tag{7.2.2}$$

The frequency where $|FB(f_x)| = 1$ is also called transit frequency f_T or cross over frequency f_x, identified by $|FB(f_x)| = 0$ dB in the amplitude diagram. The situation described in Eq. (7.2.2) corresponds to an ideal harmonic oscillator. In case we want stability rather than oscillation, we measure the degree of stability by its phase margin Φ_M (dt. Phasenreserve Φ_R) to the ideal oscillator:

$$FB = 1 \cdot e^{-180° + \Phi_M} . \tag{7.2.3}$$

In the ideal case, we would have amplifiers with infinite gain and phase shift 0°. This is not possible, so we have to come down in some way.

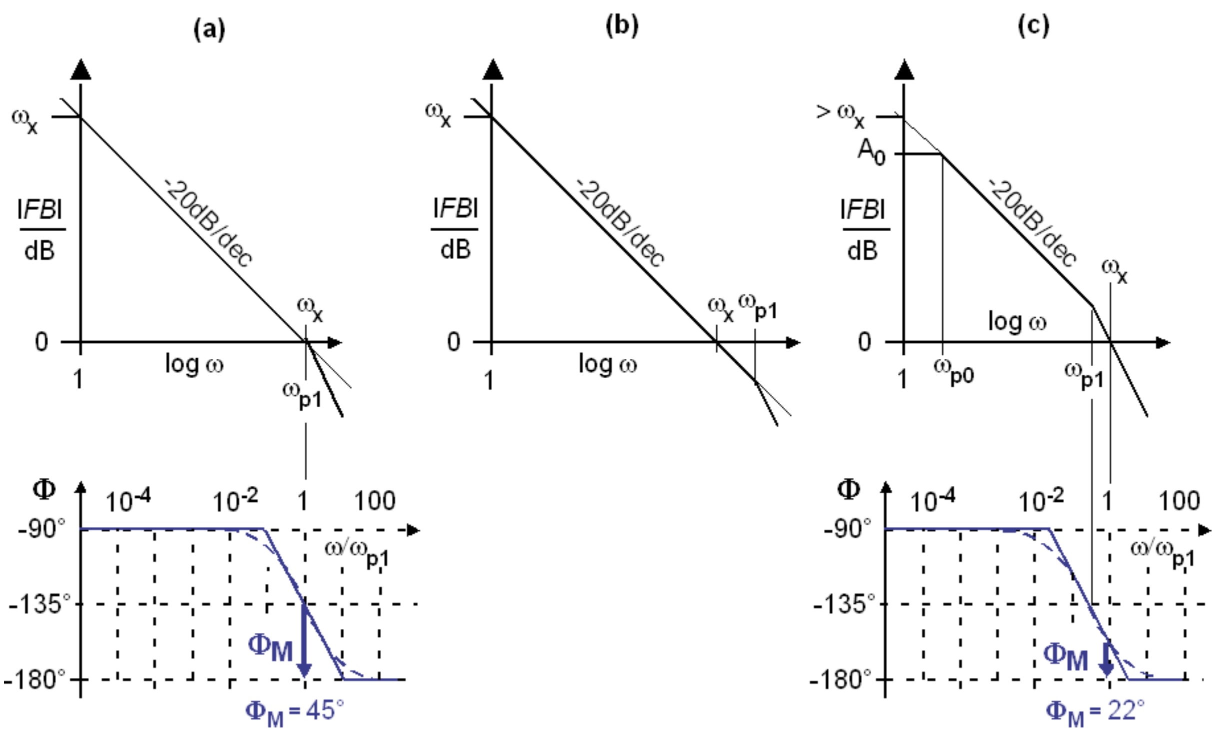

Fig. 7.2.1:. Measuring phase margin versus -180° at $|FB(\omega_x)|$=0dB: **(a)** $\omega_{p1} = \omega_x \Leftrightarrow \Phi_M = 45°$, **(b)** $\omega_{p1} > \omega_x \Leftrightarrow \Phi_M > 45°$ (not illustrated), **(c)** $\omega_{p1} < \omega_x \Leftrightarrow \Phi_M < 45°$: tends to oscillate.

7.2.2 Approaching Zero with -20dB/dec and Pole at ω_x

In Fig. 7.2.2 (a-c) we have $\omega_{p0} << \omega_{p1}$ causing -20dB/dec amplitude drop and -90° phase shift. This corresponds to a 1st order integrator. In Fig. part (c) $\omega_{p0} <$ is sketched.
We assume that higher poles $\omega_{p\#}$, #=2, 3, 4,…, are at $\omega_{p\#} >> \omega_{p1}$ having no impact on the stability criterion at crossover-0dB frequency ω_x.

(a) In Fig. part (a) $\omega_{p1a} = \omega_x$ contributes additional -45° at ω_x to the -90° phase shift of ω_{p0}, so that the total phase shift at cross-over is -135° and consequently the phase margin to -180° is $\Phi_{Ma} = 45°$. This is the rule-of-thumb case for control setting.

(b) In Fig. part (b) $\omega_{p1} > \omega_x$. Consequently, it contributes less than -45° at ω_x to the -90° phase shift of ω_{p0}, so that the total phase shift at cross-over is > -135° and consequently the phase margin to -180° is $\Phi_{Mb} > 45°$. This is more stable but slower than case (a).

(c) In Fig. part (c) $\omega_{p1} > \omega_x$. Consequently, it contributes more than -45° at ω_x to the -90° phase shift of ω_{p0}, so that the total phase shift at cross-over is < -135° and consequently the phase margin to -180° is $\Phi_{Mc} < 45°$.
In this part of the figure, maximum amplification A_0 is illustrated to create pole ω_{p0}, which is far enough below ω_x to have no impact on the stability criterion at ω_x.

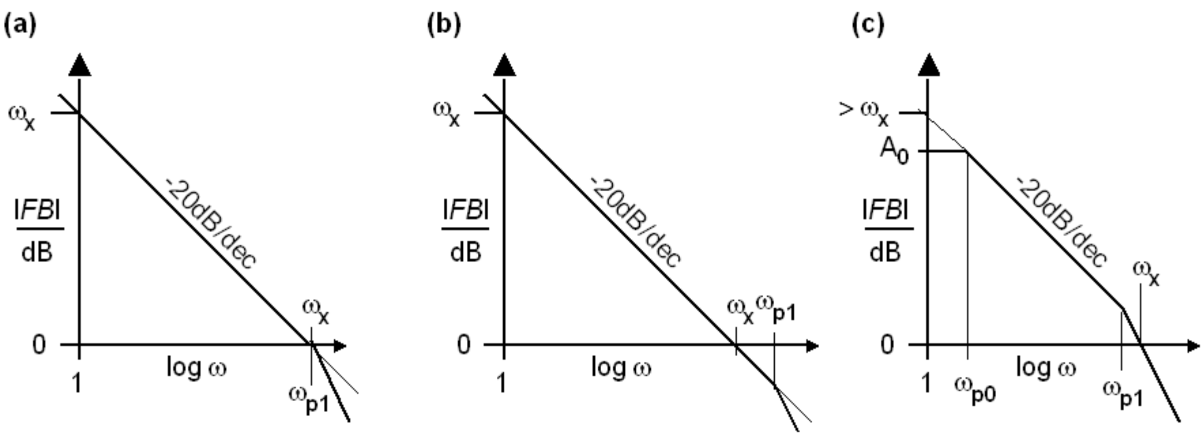

(d) Bode diagram **(e)** Step responses

Characteristics of some lowpasses: Butterworth 1st order (blue), 2nd order (red), 3rd order (yellow) ϕ_M=45 (pink).

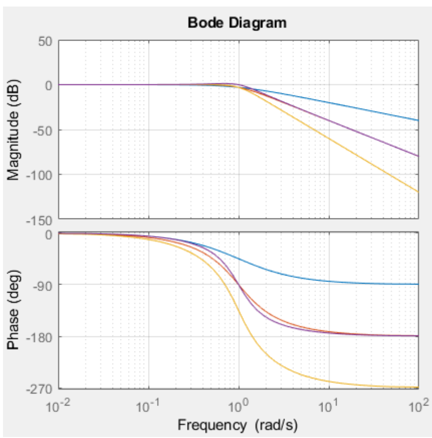

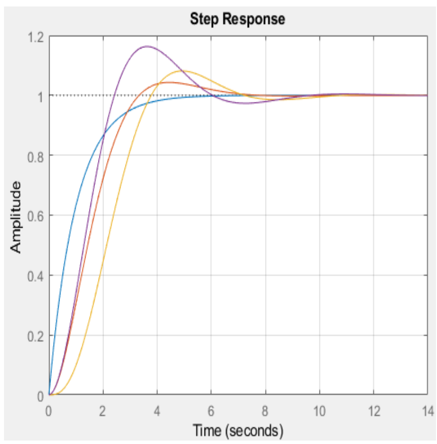

Fig. 7.2.2:. Comparing crossover frequency ω_x and pole ω_{p1} for phase margin considerations:
(a) $\omega_{p1} = \omega_x \Leftrightarrow \Phi_M = 45°$, **(b)** $\omega_{p1} > \omega_x \Leftrightarrow \Phi_M > 45°$, **(c)** $\omega_{p1} < \omega_x \Leftrightarrow \Phi_M < 45°$.
(d) frequency and **(e)** step responses to situation (a) (pink) and 2nd order *Butterworth* (red).

Fig. 7.2.2(d) and (e) compare closed-loop (*STF*) step responses obtained by different pole-setting strategies to the 1st order integrator assumed in Fig. 7.2.1.

- Stability criterion: open-loop phase-margin $\Phi_M = 45°$, (i.e. $\omega_{p1} = \omega_x$), corresponding to the pink curves in Fig. 7.2.2. The signal transfer function of the closed loop features a small peaking in the frequency domain illustrated in Fig. 7.2.2(a) and some 18% voltage overshoot to the step response in Fig. part (b).
- Stability criterion: 2nd order *Butterworth* setting for the closed loop's poles, corresponding to the red curves in Fig. 7.2.2. No peaking in the frequency domain → Fig. part (a), and some 4.29% voltage overshoot to the step response in time-domain → Fig. part (b).
- Fig. 7.2.2 illustrates the frequency and time-domain responses for a 1st (=RC lowpass) and 3rd order Butterworth filter, for completeness. They principally feature -3.01dB and no peaking in the frequency domain. Voltage overshoot to step response increases with order.

In conclusion, better results are obtained for optimizing poles of the closed loop, but the rule-of-thumb optimization t phase margin $\Phi_M = 45°$ is acceptable.

Mathematical Modeling

***FB* = 1st order Integrator:** stable. Let forward network *FB* and feedback network *B*

$$FB = \frac{\omega_x}{s} \xrightarrow{s=j\omega} \frac{\omega_x}{j\omega} = -j\frac{\omega_x}{\omega} = \frac{\omega_x}{\omega}e^{-j90°} \tag{7.2.2.1}$$

$\phi_M = 90°$ → stable.

$$STF(s) = \frac{F}{1+FB} = B^{-1}\frac{FB}{1+FB} = B^{-1}\frac{\omega_x}{s+\omega_x} \xrightarrow{s\to 0} B^{-1} \tag{7.2.2.2}$$

Fig. (a) 1st order integrator, pole $\omega_{p1} = \omega_x$. Let forward network *FB* and feedback *B* with

$$FB(s) = \frac{\omega_x}{s(1+s/\omega_{p1})} = \frac{\omega_x\omega_{p1}}{s(s+\omega_{p1})} \tag{7.2.2.3}$$

$$STF(s) = \frac{F}{1+FB} = B^{-1}\frac{FB}{1+FB} = B^{-1}\frac{\omega_x\omega_{p1}}{s^2+\omega_{p1}s+\omega_x\omega_{p1}} \xrightarrow{s\to 0} B^{-1} \tag{7.2.2.4}$$

Comparison with general 2nd order lowpass Eq. (7.1.6):

$$A_0 = B^{-1}, \tag{7.2.2.5}$$

$$D = 0.5\cdot\sqrt{\omega_{p1}/\omega_x}\ . \tag{7.2.2.6}$$

$$\omega_0^2 = \omega_{p1}\omega_x\ , \tag{7.2.2.7}$$

The $\Phi_M = 45°$ case with $\omega_{p1} = \omega_x$ yields D=1/2 while Butterworth conditions require $D = \sqrt{1/2}$, so that for ***Butterworth* conditions**

$$\boldsymbol{\omega_{p1,BW} = 2\cdot\omega_x}\ . \tag{7.2.2.8}$$

7.2.3 Approaching Zero with -40dB/dec and Zero at ω_x

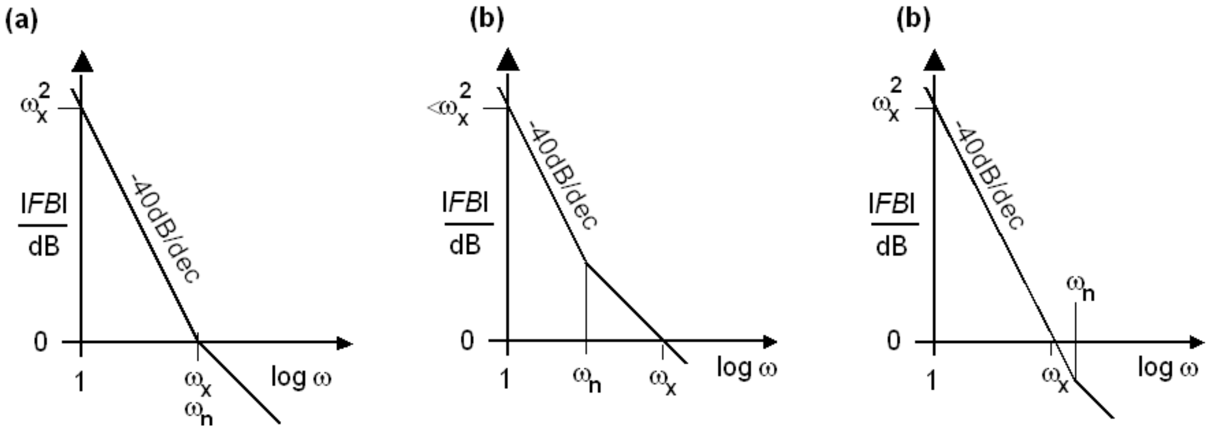

(d) Bode diagram

(e) Step responses

Characteristics of some lowpasses made with open-loop gain being a 2nd order integrator with a zero ω_n. Butterworth ϕ_M=45: yellow BW: red, aperiodic: blue.

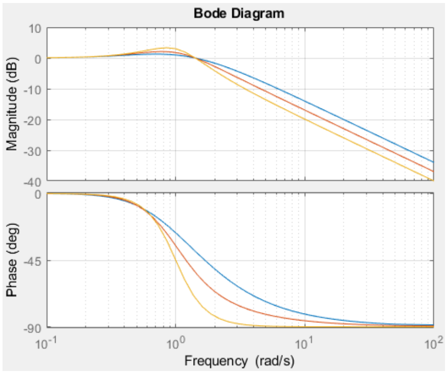

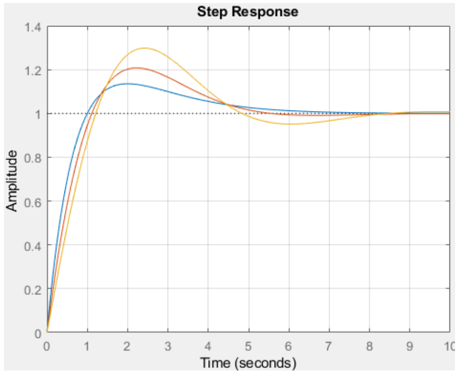

Fig. 7.2.3:. Comparing cross-over frequency ω_x and pole ω_{p2} for phase margin considerations: **(a)** $\omega_n = \omega_x \Leftrightarrow \Phi_M = 45°$, **(b)** $\omega_n < \omega_x \Leftrightarrow \Phi_M > 45°$, **(c)** $\omega_n > \omega_x \Leftrightarrow \Phi_M < 45°$; **(d)** frequency and **(e)** step responses to situation (a), (yellow) and a 2nd order *Butterworth* denominator with zero (red).

Observations:

- If *FB* is a 2nd order integrator, the closed loop is a harmonic oscillator.
- Placing a zero at ω_x to fulfil the 45° phase margin conditions yield with 30% more voltage overshoot to a step response (yellow), than placing a pole at ω_x to a 1st order integrator (18%).
- Adjusting the system to *Butterworth* poles requires $\omega_n = \omega_x / D = \sqrt{2}$, but still has some 20% voltage overshoot to a step response (orange).
- Adjusting the system to noncomplex aperiodic borderline poles requires $\omega_n = \omega_2/2$, but due to the zero the system still has some 14% voltage overshoot (orange) to a step response.

Mathematical Modeling

***FB* = 2nd order integrator:** oscillator. Let Forward network *FB* and feedback *B*

$$FB = \left(\frac{\omega_x}{s}\right)^2 \xrightarrow{s=j\omega} -\frac{\omega_x}{\omega^2} = \frac{\omega_x}{\omega^2} e^{-j180°} \qquad (7.2.3.1)$$

$\phi_M = 0°$ → ideal harmonic oscillator.

$$STF(s) = \frac{F}{1+FB} = B^{-1}\frac{FB}{1+FB} = B^{-1}\frac{\omega_x^2}{s^2+\omega_x^2} \xrightarrow{s=j\omega} B^{-1}\frac{\omega_x^2}{\omega^2+\omega_x^2} \qquad (7.2.3.2)$$

STF has a pole pair on the jω axis in $s_{p1,2} = \pm j\omega_x$ → harmonic oscillator.

Fig. (a) 2nd order integrator, zero $\omega_n = \omega_x$. Let forward network *FB* and feedback *B*

$$FB(s) = \frac{\omega_x^2}{s^2}(1+s/\omega_n) = \frac{\omega_x^2}{\omega_n}\frac{s+\omega_n}{s^2} \qquad (8.3.3)$$

$$STF(s) = \frac{F}{1+FB} = B^{-1}\frac{FB}{1+FB} = B^{-1}\frac{(\omega_x^2/\omega_n)\cdot s+\omega_x^2}{s^2+(\omega_x^2/\omega_n)\cdot s+\omega_x^2} \xrightarrow{s\to 0} B^{-1} \qquad (8.3.4)$$

Comparison with general 2nd order lowpass Eq. (7.1.6):

$$A_0 = B^{-1}, \qquad (8.3.5)$$

$$D = \frac{\omega_x}{2\omega_n}, \qquad (8.3.6)$$

$$\omega_0 = \omega_x\ . \qquad (8.3.7)$$

PM45: $\omega_n = \omega_2$. The most usual strategy is to place the zero at $\omega_n = \omega_x$. This corresponds to D=½ and consequently poles at $s_{p1,2} = -D\cdot\omega_1\cdot exp(\pm 60°)$. Together with the zero this obtains 3.3dB peeking in the frequency domain and 30% step-response voltage overshoot.

BW2: 2nd order *Butterworth* denominator: $\omega_n = \cdot\omega_x/\sqrt{2}$. This yields $D=\sqrt{1/2}$ and poles at $s_{p1,2} = -D\cdot\omega_0\cdot exp(\pm 45°)$. Together with the zero this obtains 2.1dB peeking in the frequency domain and 21% step-response voltage overshoot in time-domain.

AP2: $\omega_n = \omega_2/2$. This yields D=1 and consequently two poles at $s_{p1,2} = -\omega_2$. However, together with the zero the system is not aperiodic but features 1.3dB peeking in the frequency domain and 14% step-response voltage overshoot in time-domain.

Listing 7.2.3: Matlab code generating Fig. 7.3

```
% Filter: 2 poles, 1 zero
Hs_M45=tf([1/1 1],[1 1 1]);
Hs_BW2=tf([1/sqrt(0.5) 1],[1 sqrt(2) 1])
Hs_AP=tf([1/0.5 1],[1 2 1]);
figure(1); step(Hs_AP,Hs_BW2,Hs_M45); grid on;
figure(2); h=bodeplot(Hs_AP,Hs_BW2,Hs_M45); grid on;
%setoptions(h,'FreqUnits','Hz','PhaseVisible','on');
```

8 Applications

8.1 *RLC* Lowpass as 2nd Order System

8.1.1 System Setup

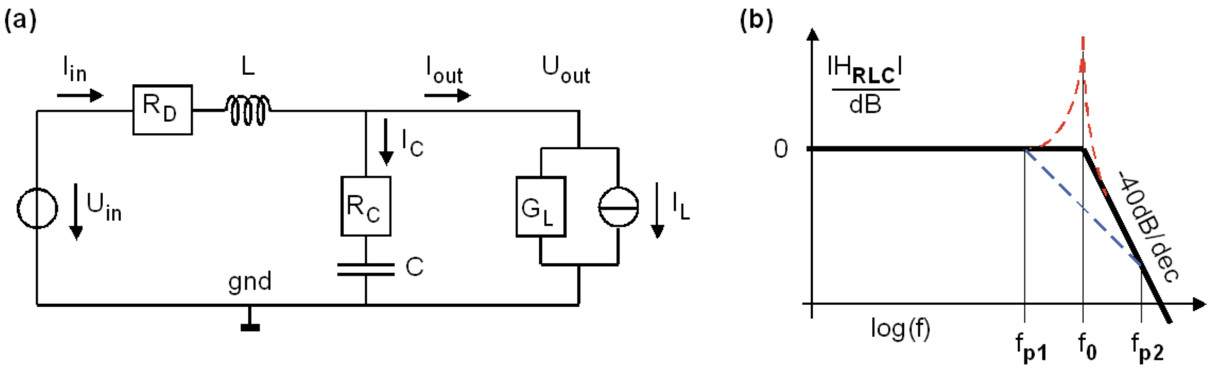

Fig. 7.4.1: (a) *RLC* lowpass **(b)** corresponding Bode diagram.

The *RLC* lowpass shown in Fig. 7.4.1 is important for DC/DC converters. It is good-natured with respect to both low and high frequencies, but may show instabilities around f_0 and within control loops.

R_C is the equivalent series resistance (ESR) of capacitor C and R_D is the wire resistance of the inductor in series with the voltage source output impedance. In the two subsections below will compute LTI model of Fig. 7.4.1

1. In the polynomial coefficients of $\dfrac{a_0 + a_1 s + a_2 s^2}{b_0 + b_1 s + b_2 s^2}$

2. as standard 2nd order model $\dfrac{A_0 \cdot \omega_0^2 (1 + s/\omega_{n1})(1 + s/\omega_{n2})}{s^2 + 2D\omega_0 \cdot s + \omega_0^2}$

Both has to be done for process transfer function *PTF* (or short H_P) computing output voltage U_{out} as function of input voltage U_{in} :

$$PTF(s) = \left.\frac{U_{out}}{U_{in}}\right|_{I_L=0} , \tag{8.1.1}$$

and inference (quarrel) transfer function respecting the impact of inference I_L on U_{out} as

$$QTF(s) = \left.\frac{U_{out}}{-I_L}\right|_{U_{in}=0} , \tag{8.1.2}$$

so that

$$U_{out}(s) = PTF(s)\cdot U_{in}(s) + QTF(s)\cdot I_L(s)\ . \tag{8.1.3}$$

According to the appendix we get

$$PTF(s) = \frac{U_{out}}{U_{in}} = \frac{1 + CR_C\cdot s}{1 + R_D G_L + \big((R_C + R_D + R_D R_C G_L)C + G_L L\big)\cdot s + (1 + R_C G_L)LC\cdot s^2}\ , \tag{8.1.4}$$

$$QTF = \frac{U_{out}}{-I_L} = \frac{-R_D(1 + sCR_C)(1 + sL/R_D)}{1 + R_D G_L + \big((R_C + R_D + R_D R_C G_L)C + G_L L\big)\cdot s + (1 + R_C G_L)LC\cdot s^2}\ . \tag{8.1.5}$$

8.1.2 Modelling the RLC Lowpass with 2nd Order Polynomials Ansatz

Ansatz

$$PTF(s) = \left.\frac{U_{out}}{U_{in}}\right|_{I_L=0} = \frac{a_{p0} + a_{p1}s + a_{p2}s^2}{b_{p0} + b_{p1}s + b_{p2}s^2} \tag{8.1.6}$$

Delivers

(8.1.7)

$a_{p0} = 1$ $\qquad a_{p1} = C\cdot R_C$ $\qquad a_{p2} = 0$

$b_{p0} = 1 + R_D G_L$ $\qquad b_{p1} = (R_C + R_D + R_D R_C G_L)C + G_L L$ $\qquad b_{p2} = (1 + R_C G_L)LC$

Ansatz

$$QTF(s) = \left.\frac{U_{out}}{-I_L}\right|_{U_{in}=0} = \frac{a_{q0} + a_{q1}s + a_{q2}s^2}{b_{q0} + b_{q1}s + b_{q2}s^2} \tag{8.1.8}$$

Delivers

(8.1.9)

$a_{q0} = -R_D$ $\qquad a_{q1} = -(R_C R_D C + L)$ $\qquad a_{q2} = -R_C LC$

$b_{q0} = b_{p0}$ $\qquad b_{q1} = b_{p1}$ $\qquad b_{q2} = b_{p2}$

8.1.3 Modelling the RLC Lowpass as Standard 2nd Order System

Process transfer function in the standard 2nd order system ansatz

$$PTF(s) = \left.\frac{U_{out}}{U_{in}}\right|_{I_L=0} = \frac{A_0\cdot\omega_0^2(1 + s/\omega_{n1})}{s^2 + 2D\omega_0\cdot s + \omega_0^2} \tag{8.1.10}$$

with a zero in ω_{n1} and poles – depending on $|D|>1$ or <1 – in

$$s_{p1,2} = -\omega_0\left(D \pm \sqrt{D^2-1}\right) = -\omega_0\left(D \pm j\sqrt{1-D^2}\right) \tag{8.1.11}$$

delivers

$$A_0 = \frac{1}{1+R_D G_L} \xrightarrow{R_D G_L \to 0} 1 \tag{8.1.12}$$

$$\omega_{n1} = \frac{1}{R_C C} \tag{8.1.13}$$

$$\omega_0 = \sqrt{\frac{1+R_D G_L}{1+R_C G_L}\cdot\frac{1}{LC}} \xrightarrow{R_C, R_D, G_L \to 0} \sqrt{\frac{1}{LC}} \tag{8.1.14}$$

$$D_D = \frac{R_D + R_C + R_D R_C G_L}{2\sqrt{(1+R_D G_L)(1+R_C G_L)}}\sqrt{\frac{C}{L}} \xrightarrow{R_C, R_D, G_L \to 0} \frac{R_D + R_C}{2}\sqrt{\frac{C}{L}} \tag{8.1.15}$$

$$D_L = \frac{G_L}{2\sqrt{(1+R_D G_L)(1+R_C G_L)}}\sqrt{\frac{L}{C}} \xrightarrow{R_C, R_D, G_L \to 0} \frac{G_L}{2}\sqrt{\frac{L}{C}} \tag{8.1.16}$$

$$D = D_D + D_L \xrightarrow{R_C, R_D, G_L \to 0} \frac{R_D + R_C}{2}\sqrt{\frac{C}{L}} + \frac{G_L}{2}\sqrt{\frac{L}{C}} \tag{8.1.17}$$

Inference (quarrel) transfer function modelling the impact of inference I_L on U_{out} with ansatz

$$QTF(s) = \left.\frac{U_{out}}{-I_L}\right|_{U_{in}=0} = \frac{-R_D A_0 \cdot \omega_0^2 (1+s/\omega_{n1})(1+s/\omega_{n2})}{s^2 + 2D\omega_0 \cdot s + \omega_0^2} \tag{8.1.18}$$

has the same denominator and ω_{n1} as $PTF(s)$, but a second zero at

$$\omega_{n2} = R_D / L \tag{8.1.19}$$

and DC impedance

$$R_0 = A_0 R_D \ . \tag{8.1.20}$$

It is seen that

$$QTF(s) = -R_D(1+s/\omega_{n2}) \cdot PTF(s) . \tag{8.1.21}$$

8.2 PID Controller as 2[nd] order System

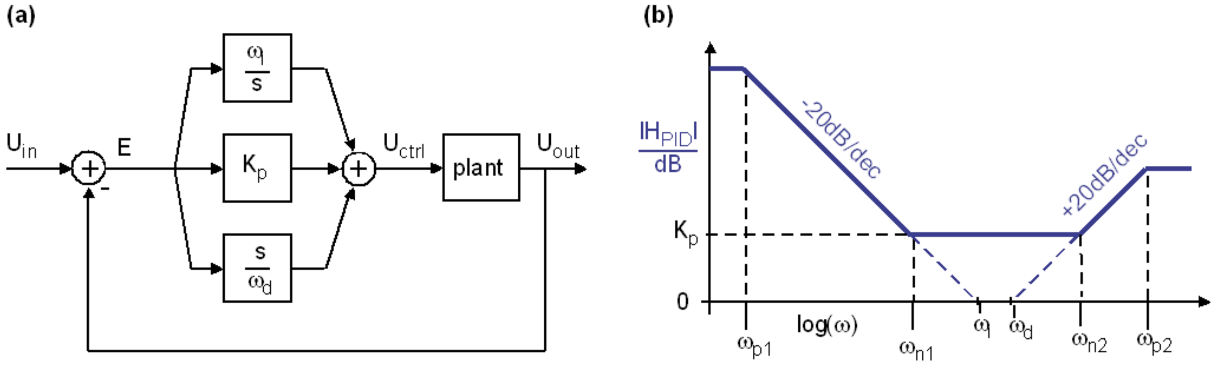

Fig. 7.5: (a) PID controller and (b) its Bode diagram: amplify both low and high frequencies.

General bi-quadratic polynomial description is

$$H_{spid}(s) = \frac{a_{0pid} + a_{1pid}s + a_{2pid}s^2}{b_{0pid} + b_{1pid}s + b_{2pid}s^2} \qquad \rightarrow \qquad H_{zpid}(z) = \frac{d_{0pid} + d_{1pid}z^{-1} + d_{2pid}z^{-2}}{1 + c_{1pid}z^{-1} + c_{2pid}z^{-2}}$$

8.2.1 Controller Transfer Function Defined by K_P, K_I, K_D, ω_{p2}

K_P, K_I, K_D : Controller engineers model PID controllers typically as

$$CTF = \frac{C(s)}{E(s)} = K_P + \frac{K_I}{s} + K_D \cdot s = \frac{K_I + K_P \cdot s + K_I \cdot s^2}{s} \tag{8.2.1}$$

with K_P, K_I, K_D being proportional, integral and derivative control parameters.

Additional Pole ω_{p1} : In practical applications infinite integrator amplification is often not possible, so the we have an unintentional pole ω_{p1} in the integral part, like $K_I/(s+\omega_{p1})$ limiting its maximum amplification to $K_I \cdot\omega_{p2} / \omega_{p1}$ as detailed in (8.2.4).

Additional Pole ω_{pd} : For control stability we frequently need also a pole for the derivative part, so that $K_D{\cdot}s$ becomes $K_D{\cdot}s/(1+s/\omega_{pd}) = K_D{\cdot}s/(1+s{\cdot}\tau_{pd})$ with $\tau_{pd} = 1/\omega_{pd}$.

Additional Pole ω_{pi} : As infinite amplification is hardly possible, we typically get a de-facto pole in the integrator, that can e modeled as $K_I / (s+\omega_{pi})$. The designer has nothing to do to build pole ω_{pi}, it arises inavoidably (and unwanted) from limited integrator amplification:

$$CTF = \frac{C(s)}{E(s)} = K_P + \frac{K_I}{s+\omega_{pi}} + K_D \cdot \frac{s}{1+s\cdot\omega_{pd}} \tag{8.2.2}$$

$$CTF = \frac{C(s)}{E(s)} = \frac{\left(K_I + K_P\omega_{pi}\right) + \left(K_P(1+\omega_{pi}\tau_{pd}) + K_I\tau_{pd} + K_D\omega_{pi}\right)\cdot s + \left(K_D + K_P\tau_{pd}\right)\cdot s^2}{\omega_{pi} + (1+\omega_{pi}\tau_{pd})\cdot s + \tau_{pd}\cdot s^2}$$

Ansatz $CTF(s) = \dfrac{a_{c0} + a_{c1} \cdot s + a_{c2} \cdot s^2}{b_{c0} + b_{c1} \cdot s + b_{c2} \cdot s^2}$ delivers

$$a_{c0} = K_I \cdot \omega_{p2} \qquad a_{c1} = K_I + K_P \cdot \omega_{p2} \qquad a_{c2} = K_P + K_D \cdot \omega_{p2} \tag{8.2.3}$$
$$b_{c0} = 0 \qquad b_{c1} = \omega_{p2} \qquad b_{p2} = 1$$

DC amplification according to (8.2.3) is $CTF(s=0) = a_{c0}/b_{c0} \to \infty$. In reality, the maximum controller amplification is limited, e.g. by the DC amplification of an operational amplifier. Parameter b_{c0} can be used to model a realistic DC amplification by

$$b_{c0} = a_{c0} \,/\, CTF(s{=}0) = K_I \cdot \omega_{p2} \,/\, \omega_{p1}. \tag{8.2.4}$$

Table 7.5.2: Matlab's designations and symbols for controller parameters

***Matlab* parameter designations**	***Matlab* symbol**	**Author's symbol**
Proportional controller parameter	K_P	K_P
Integral controller parameter	I	K_I
Derivative controller parameter	D	K_D
Filter coefficient	N	ω_{p2}

8.2.2 Controller Transfer Function Defined by K_P, ω_{n1}, ω_{n2}, ω_{p1}, ω_{p2}

Ansatz:

$$H_{PID}(s) = const \cdot \frac{(s+\omega_{n1})(s+\omega_{n2})}{(s+\omega_{p1})(s+\omega_{p2})} = Kp \cdot \frac{\dfrac{\omega_{n1}\omega_{n2}}{\omega_{n1}+\omega_{n2}} + s + \dfrac{1}{\omega_{n1}+\omega_{n2}} s^2}{\dfrac{\omega_{p1}\omega_{p2}}{\omega_{p1}+\omega_{p2}} + s + \dfrac{1}{\omega_{p1}+\omega_{p2}} s^2} \tag{8.2.5}$$

Comparing it to

$$H_{PID}(s) = \frac{a_0 + a_1 s + a_2 s^2}{b_0 + b_1 s + b_2 s^2} \tag{8.2.6}$$

delivers

$$a_0 = K_p \frac{\omega_{n1}\omega_{n2}}{\omega_{n1}+\omega_{n2}}, \qquad a_1 = K_p, \qquad a_2 = \frac{K_p}{\omega_{n1}+\omega_{n2}}, \tag{8.2.7}$$

$$b_0 = \frac{\omega_{p1}\omega_{p2}}{\omega_{p1}+\omega_{p2}}, \qquad b_1 = 1, \qquad b_2 = \frac{1}{\omega_{p1}+\omega_{p2}}. \tag{8.2.8}$$

8.2.3 Translation to Time-Discrete Transfer Function

Translation to the time-discrete domain yields

$$H_{PID}(z) = \frac{d_0 + d_1 z + d_2 z^2}{1 + c_1 z + c_2 z^2} \tag{8.2.9}$$

Listing 7.5.3: Function *f_c2d_bilin* translating $s \rightarrow z$ using bi-linear substitution acc. to chap. 5.

```
function Hz = f_c2d_bilin_order2(Hs,T)
%
fs2=2/T;
a0=Hs(1,1); a1=Hs(1,2); a2=Hs(1,3);
if size(Hs,1)==1;
  b0=1; b1=0; b2=0;
else
  b0=Hs(2,1); b1=Hs(2,2); b2=Hs(2,3);
end;
as0=a0; as1=a1*fs2; as2=a2*fs2*fs2;
bs0=b0; bs1=b1*fs2; bs2=b2*fs2*fs2;
cs0=bs0+bs1+bs2; cs1=2*(bs0-bs2); cs2=bs0-bs1+bs2;
ds0=as0+as1+as2; ds1=2*(as0-as2); ds2=as0-as1+as2;
Hz = [[ds0 ds1 ds2];[cs0 cs1 cs2]];
if cs0~=1; Hz=Hz/cs0; end;
```

8.2.4 Exercise

How does *Matlab's* filter coefficient *N* in the *PID* controller equation depend on the *PID* parametes detailed above?

Solution exercise 7.5: $N = \omega_{p2}$.

8.3 Time-Continuous Filter using Integrotors

8.3.1 Linearization of a Time-Continuous Integrator: Offset Removal

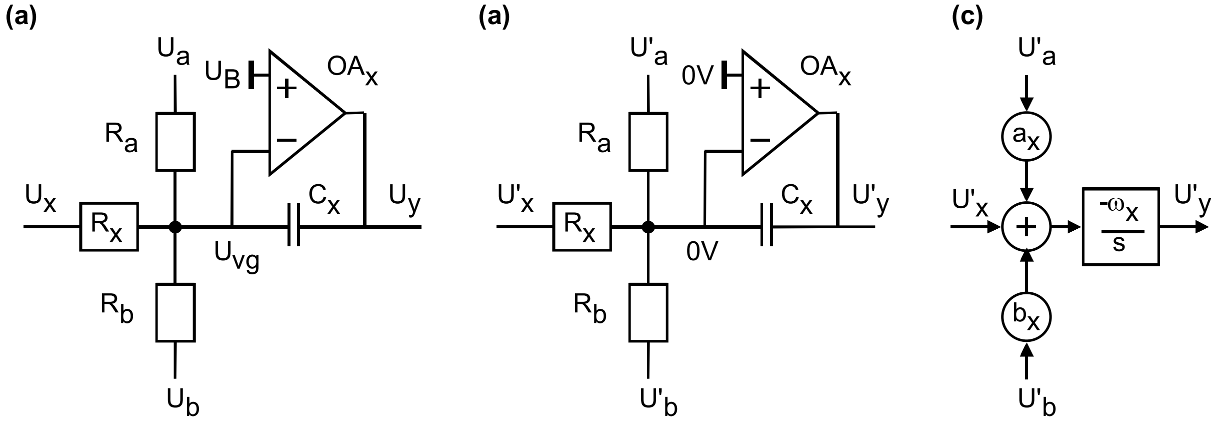

Fig. 8.3.1: (a) Real Situation, **(b)** circuit linearized, **(c)** equivalent signal-flow model.

First of all we have to linearize the circuit. Assume a 3-input integrator as shown in part (a) of the figure above. Its behavior is described by

$$U_{out} - U_{vg} = -\frac{U_a - U_{vg}}{sR_aC_x} - \frac{U_x - U_{vg}}{sR_xC_x} - \frac{U_b - U_{vg}}{sR_bC_x} \qquad (8.3.1)$$

where the virtual ground voltage U_{vg} is given by $U_{vg} = U_B - U_{off} - U_{out} / A_V$ (8.3.2)

with A_V being the OpAmp's amplification. To linearize (8.3.1) we have to remove the constant term, i.e. U_B-U_{off}. The amplifier's offset voltage, U_{off}, is either compensated for or neglected assuming $U_{off}\approx$0V. To remove U_B we remember that any voltage in the circuit can be defined to be reference potential, i.e. 0V, and define

$U' = U - U_B$ (8.3.3) $\Leftrightarrow$ $U = U' + U_B$ (8.3.4)

This yields the circuit in Fig. part (b) which is linear in the sense of (2.1). Things are facilitated assuming also Av→∞ so that U_{vg}=U_B so that U'_{vg}=0V. Then (8.3.1) facilitates to

$$U'_{out} = -\frac{U'_a}{sR_aC_x} - \frac{U'_x}{sR_xC_x} - \frac{U'_b}{sR_bC_x} \qquad (8.3.5)$$

It is always possible to factor out coefficients such, that the weight of one input is one, e.g.

$$U'_{out} = \left(aU'_a + U'_x + bU'_b\right)\cdot\left[\frac{-\omega_x}{s}\right] \qquad (8.3.7) \qquad \text{with} \qquad \omega_x = \frac{1}{R_xC_k} \qquad (8.3.7)$$

$$a = \frac{R_x}{R_a} \qquad (8.3.8) \qquad \text{and} \qquad b = \frac{R_x}{R_b} \qquad (8.3.9)$$

8.3.2 Application to a Time-Continuous 1st-Order System

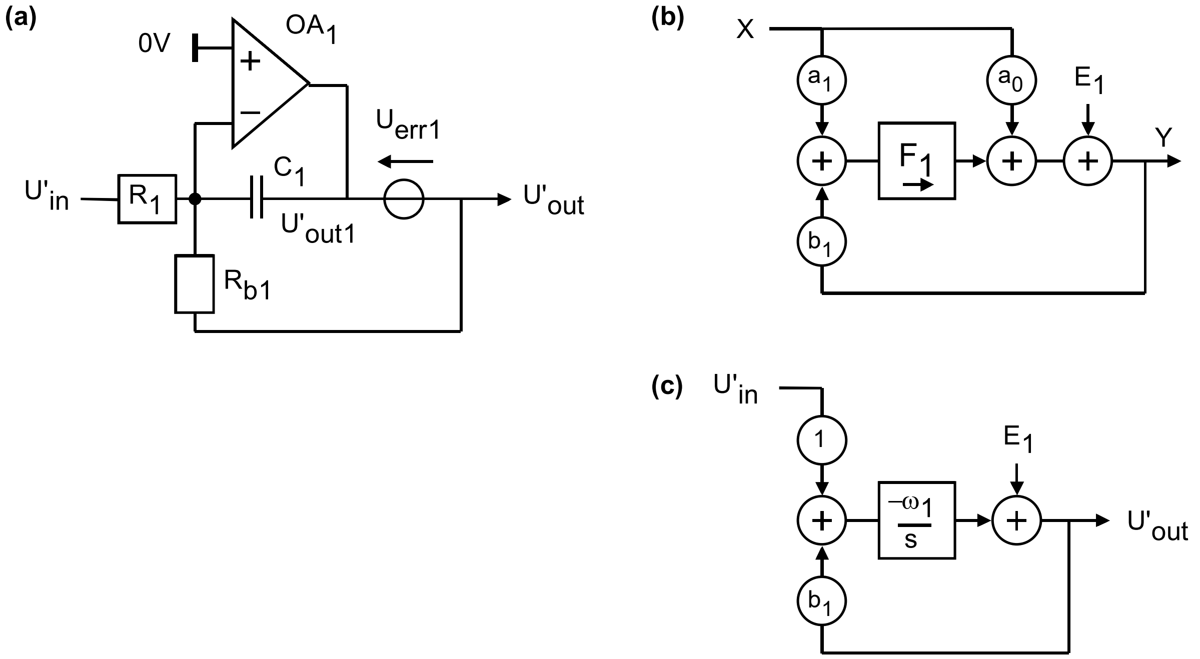

Fig. 8.3.2: (a) Real Circuit, **(b)** general model, **(c)** particular model for circuit in (a).

Fig. 8.3.2 (a) shows the analog circuit under consideration. Fig. part (b) illustrates the very general form of the topology. To get forward network A set $b_1=E_1=0$. Identify all paths a signal can take from X to Y. Assuming a linear system the sum of all those partial transfer function delivers the STF. Open-loop network B is found by summing all paths from Y to Y:

$$A=\left.\frac{Y}{X}\right|_{E_1=b_1=0}=a_0+a_1F_1\ , \qquad (8.3.10) \qquad\qquad B=\left.\frac{Y}{Y}\right|_{X=0}=b_1F_1 \qquad (8.3.11)$$

Adapting the general topology in part (b) to the particular model in Fig. part (c) we can select either a_k or b_k free. Let's set a_k=1. Here, with order k=1, we get

$$a_1=1\ ,\quad a_0=0\ ,\quad b_1=\frac{R_1}{R_{b1}}\ ,\quad \omega_1=\frac{1}{R_1C_1}\ ,\quad F_1=-\frac{\omega_1}{s} \qquad (8.3.12)$$

Signal and noise transfer functions can then be computed from

$$STF=\frac{A}{1-B}=\frac{a_0+a_1F_1}{1-b_1F_1}=\frac{F_1}{1-F_1}=\frac{(-\omega_1/s)}{1-b_1(-\omega_1/s)}=-\frac{\omega_1}{s+b_1\omega_1}.$$

Hence :

$$\boxed{STF=-\frac{\omega_1}{s+b_1\omega_1}=-\frac{R_{b1}}{R_1}\frac{1}{1+sR_{b1}C_1}\xrightarrow{s\to 0}-\frac{1}{b_1}=-\frac{R_{b1}}{R_1}} \qquad (8.3.13)$$

$$NTF=\frac{1}{1-B}=\frac{1}{1-b_1F_1}=\frac{1}{1-b_1(-\omega_1/s)} \quad => \quad \boxed{NTF=\frac{s}{s+b_1\omega_1}=\frac{sR_{b1}C_1}{1+sR_{b1}C_1}\xrightarrow{s\to 0}0} \qquad (8.3.14)$$

8.3.3 Application to a Time-Continuous 2nd-Order System

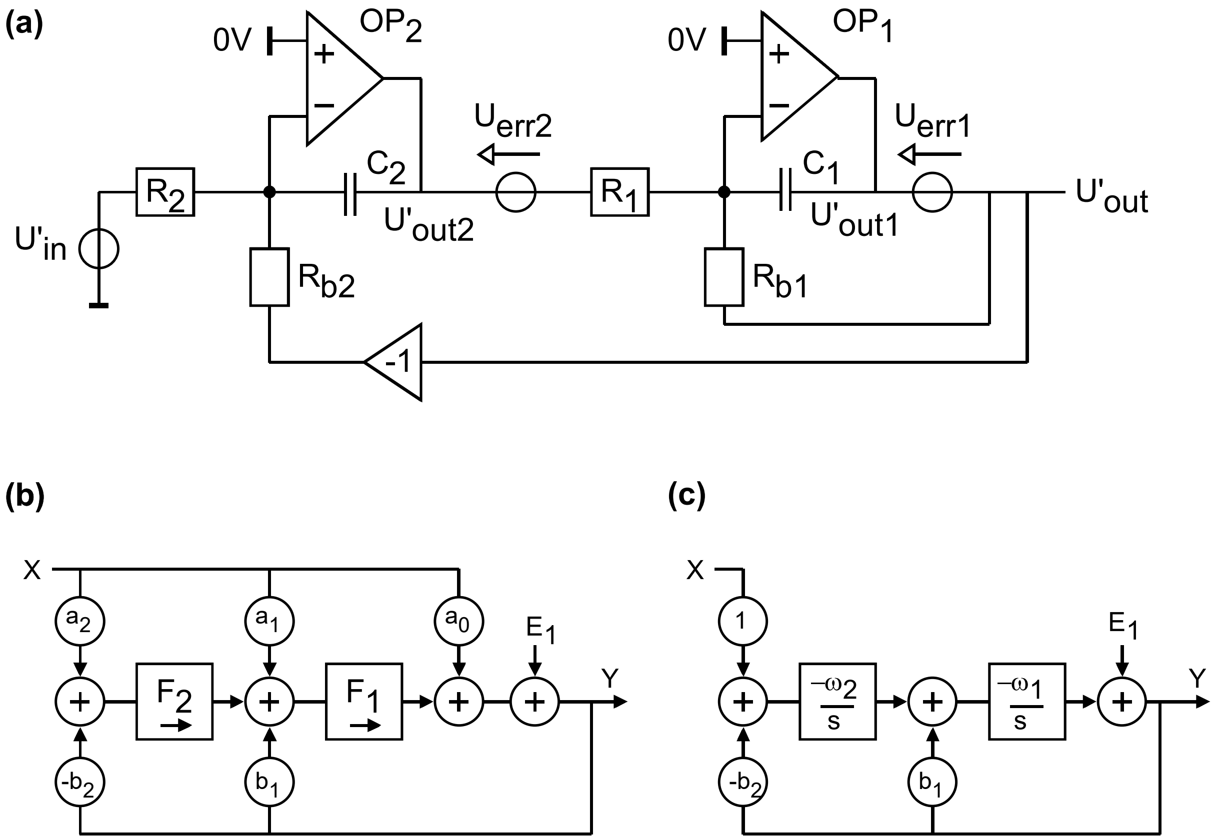

Fig. 8.3.3: (a) Real Circuit, **(b)** general model, **(c)** particular model for circuit in (a).

Fig. 8.3.3 (a) shows the analog circuit under consideration. Fig. part (b) illustrates the very general form of the topology. To get forward network A set $b_1=b_2=E_1=0$. Identify all paths a signal can take from X to Y. Assuming a linear system the sum of all those partial transfer function delivers the STF. Open-loop network B is found by summing all paths from Y to Y:

$$A=\left.\frac{Y}{X}\right|_{E_1=b_1=b_2=0}=a_0+a_1F_1+a_2F_1F_2\ , \qquad (8.3.15) \qquad\qquad B=\left.\frac{Y}{Y}\right|_{X=0}=b_1F_1-b_2F_1F_2 \quad (8.3.17)$$

Adapting the general topology in part (b) to the particular model in Fig. part (c) we can select either a_k or b_k free. Let's set a_k=1. Here, with order k=2, we get

$$a_2=1,\ \ a_1=a_0=0,\ \ b_2=\frac{R_2}{R_{b2}},\ \ b_1=\frac{R_1}{R_{b1}},\ \ \omega_2=\frac{1}{R_2C_2},\ \omega_1=\frac{1}{R_1C_1},\ \ F_2=-\frac{\omega_2}{s},\ \ F_1=-\frac{\omega_1}{s}$$

(8.3.17)

The signal transfer function can then be computed from

$$STF = \frac{A}{1-B} = \frac{a_0 + a_1F_1 + a_2F_2F_1}{1 - b_1F_1 - (-b_2F_2F_1)} = \frac{F_2F_1}{1 - b_1F_1 + b_2F_2F_1} = \frac{\frac{-\omega_1}{s}\frac{-\omega_2}{s}}{1 - b_1\frac{-\omega_1}{s} + b_2\frac{-\omega_1}{s}\frac{-\omega_2}{s}} \Rightarrow$$

$$\boxed{STF = \frac{\omega_1\omega_2}{s^2 + b_1\omega_1 s + b_2\omega_1\omega_2}} \tag{8.3.18}$$

We compare this result to the general 2nd-order model $\boxed{H_{2ndOrder} = \frac{A_0\omega_0^2}{s^2 + 2D\omega_0 s + \omega_0^2}}$ (8.3.19)

with DC amplification A_0, cutoff frequency ω_0 and damping constant *D*. (8.3.18)=(8.3.19) delivers

$$STF = \frac{\omega_1\omega_2}{s^2 + b_1\omega_1 s + b_2\omega_1\omega_2} = \frac{A_0\omega_0^2}{s^2 + 2D\omega_0 s + \omega_0^2} = H_{2ndOrder}$$

Comparing coefficients of *s* delivers for DC amplification, cutoff frequency, damping factor

$\boxed{A_0 = \frac{1}{b_2} = \frac{R_{b2}}{R_2}}$ (30) $\boxed{\omega_0 = \sqrt{b_2\omega_1\omega_2} = \frac{1}{\sqrt{R_1C_1R_{b2}C_2}}}$ (31) $\boxed{D = \frac{b_1\omega_1}{2\omega_0} = \frac{\sqrt{R_1R_{b2}}}{2R_{b1}}\sqrt{\frac{C_2}{C_1}}}$

(8.3.20)

The noise transfer function is computed from

$$NTF = \frac{1}{1-B} = \frac{1}{1 - b_1F_1 - (-b_2F_2F_1)} = \frac{1}{1 - b_1F_1 + b_2F_2F_1} = \frac{1}{1 - b_1\frac{-\omega_1}{s} + b_2\frac{-\omega_1}{s}\frac{-\omega_2}{s}} = \frac{s^2}{s^2 + b_1\omega_1 s + b_2\omega_1\omega_2}$$

Hence : $$NTF = \frac{s^2}{s^2 + b_1\omega_1 s + b_2\omega_1\omega_2} = \frac{s^2}{s^2 + 2D\omega_0 s + \omega_0^2} \xrightarrow{s\to 0} 0^2 \tag{8.3.21}$$

9 Conclusions

A feedback loop model valid for time-continuous and time-discrete domain modeling was derived, discussed and applied to different circuit topologies. Translation methods from s → z domain were introduced, stability issues addressed. At the several practical applications are presented.

10 References

[1] Matlab, available: https://de.mathworks.com

11 Appendices

11.1

11.2

11.3

11.4 RLC Lowpass as 2nd Order System

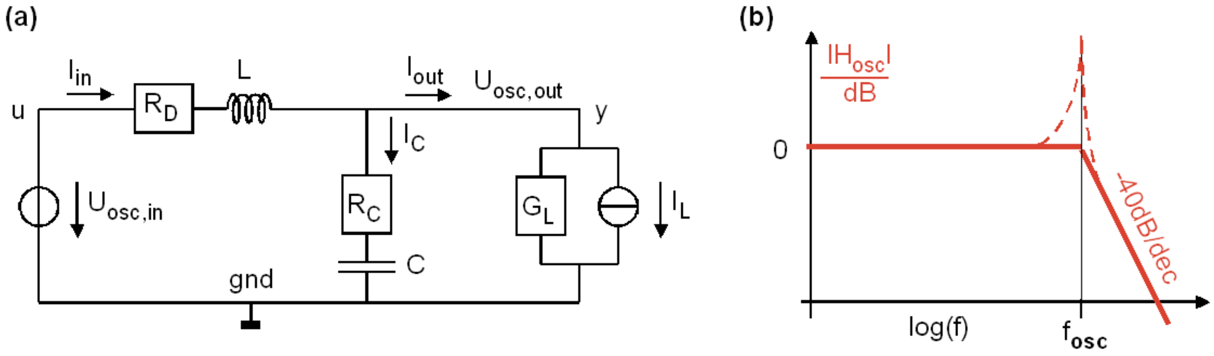

Fig. 7.4.1: **(a)** *RLC* circuit, **(b)** corresponding Bode diagram.

The *RLC* lowpass shown in Fig. 7.4.1 is important for DC/DC converstêrs. It is good-natured with respect to both low and high frequencies, but may show instabilities in its oscillation frequency and within control loops.

R_C is the equivalent series resistance (ESR) of capacitor C and R_D is the wire resistance of the inductor in series with the voltage source output impedance. In the two subsections below will compute LTI model of Fig. 7.4.1

1. In the polynomial coefficients of $\dfrac{a_0 + a_1 s + a_2 s^2}{b_0 + b_1 s + b_2 s^2}$

2. as standard 2nd order model $\dfrac{A_0 \cdot \omega_0^2 (1 + s/\omega_{n1})(1 + s/\omega_{n2})}{s^2 + 2D\omega_0 \cdot s + \omega_0^2}$

Both has to be done for process transfer function *PTF* (or short H_P) coputing output voltage U_{out} as function of input voltage U_{in} :

$$PTF(s) = \left. \frac{U_{out}}{U_{in}} \right|_{I_L = 0} ,$$

and inference (quarrel) transfer function respectings the impact of inference I_L on U_{out} as

$$QTF(s) = \left. \frac{U_{out}}{-I_L} \right|_{U_{in} = 0} ,$$

so that

$$U_{out}(s) = PTF(s) \cdot U_{in}(s) + QTF(s) \cdot I_L(s)$$

11.4.1 Computing the Laplace Transform of the Oscillator

We define

$$Z_D = R_D + sL$$

$$Z_C = R_C + \frac{1}{sC} = \frac{1+sCR_C}{sC}$$

$$Z_{CL} = \frac{1}{G_L} \parallel Z_C = \frac{Z_C}{1+G_L Z_C} = \frac{\frac{1+sCR_C}{sC}}{1+G_L\frac{1+sCR_C}{sC}} = \frac{1+sCR_C}{sC+G_L+sCG_LR_C} = \frac{1+sCR_C}{G_L+sC(1+G_LR_C)}$$

Then

$$PTF = \left.\frac{U_{out}}{U_{in}}\right|_{I_L=0} = \frac{Z_{CL}}{Z_D+Z_{CL}}$$

$$QTF = \left.\frac{U_{out}}{-I_{out}}\right|_{U_{in}=0} = Z_D \parallel Z_{CL}\,,$$

Consequently,

$$PTF(s) = \frac{U_{out}}{U_{in}} = \frac{Z_{CL}}{Z_{CL}+Z_D} = \frac{\frac{1+sCR_C}{G_L+sC(1+G_LR_C)}}{\frac{1+sCR_C}{G_L+sC(1+G_LR_C)}+(R_D+sL)}$$

$$= \frac{1+sCR_C}{1+sCR_C+(R_D+sL)\big(G_L+sC(1+G_LR_C)\big)}$$

$$= \frac{1+sCR_C}{1+sCR_C+R_DG_L+sCR_D(1+G_LR_C)+sLG_L+s^2LC(1+G_LR_C)}$$

$$= \frac{1+sR_CC}{1+R_DG_L+sR_CC+sR_DC(1+R_CG_L)+sLG_L+s^2LC(1+R_CG_L)}$$

$$= \frac{1+CR_C\cdot s}{1+R_DG_L+\big((R_C+R_D+R_DR_CG_L)C+G_LL\big)\cdot s+(1+R_CG_L)LC\cdot s^2}$$

The impact of load current I_L is modelled easily as $QTF = STF\cdot Z_D$:

$$QTF = \frac{U_{out}}{-I_L} = \frac{Z_{CP}\cdot Z_D}{Z_{CP}+Z_D} = \frac{-R_D(1+sCR_C)(1+sL/R_D)}{1+R_DG_L+\big((R_C+R_D+R_DR_CG_L)C+G_LL\big)\cdot s+(1+R_CG_L)LC\cdot s^2}$$

11.4.2 Modelling the Oscillator with 2nd Order Polynomials

Ansatz

$$PTF(s) = \frac{U_{out}(s)}{U_{in}(s)} = \frac{a_{p0} + a_{p1}s + a_{p2}s^2}{b_{p0} + b_{p1}s + b_{p2}s^2}$$

for the process transfer function delivers

$$a_{p0} = 1 \qquad a_{p1} = R_C C \qquad a_{p2} = 0$$
$$b_{p0} = 1 + R_D G_L \qquad b_{p1} = (R_C + R_D + R_D R_C G_L)C + G_L L \qquad b_{p2} = (1 + R_C G_L)LC$$

Ansatz

$$QTF(s) = Z_{osc}(s) = \frac{a_{q0} + a_{q1}s + a_{q2}s^2}{b_{q0} + b_{q1}s + b_{q2}s^2}$$

For the inference (quarrel) transfer function delivers

$$a_{osc,0} = R_W \qquad a_{osc,1} = CR_C R_D + L \qquad a_{osc,2} = R_C LC$$
$$b_{q0} = b_{p0} \qquad b_{q1} = b_{p1} \qquad b_{q2} = b_{p2}$$

11.4.3 Modelling the Oscillator as 2nd Order System

Process transfer function modelling the impact of input voltage U_{in} on U_{out}

$$PTF(s) = \left.\frac{U_{out}}{U_{in}}\right|_{I_L=0} = \frac{A_0 \cdot \omega_0^2 (1 + s/\omega_{n1})}{s^2 + 2D\omega_0 \cdot s + \omega_0^2}$$

with a zero in ω_{n1} and poles in

$$s_{p1,2} = -\omega_0 \left(D \pm j\sqrt{1-D^2} \right) .$$

delivers

$$A_0 = \frac{1}{1 + R_D G_L} \xrightarrow{R_D G_L \to 0} 1$$

$$\omega_{n1} = \frac{1}{R_C C}$$

$$PTF = \left.\frac{U_{out}}{U_{in}}\right|_{I_L=0} = \frac{\frac{1}{1+R_D G_L}\left(1+sCR_C\right)}{1+\frac{G_L L+(R_C+R_D+R_D R_C G_L)C}{1+R_D G_L}\cdot s+\frac{1+R_C G_L}{1+R_D G_L}LC\cdot s^2}$$

$$= \frac{\frac{1}{1+R_W G_L}\left(1+sCR_C\right)}{1+\frac{(R_C+R_D+R_D R_C G_L)C+G_L L}{\sqrt{(1+R_D G_L)(1+R_C G_L)}}\sqrt{\frac{1+R_C G_L}{1+R_D G_L}LC}\cdot s+\frac{1+R_C G_L}{1+R_D G_L}LC\cdot s^2}$$

$$= \frac{\frac{1}{1+R_D G_L}\left(1+sCR_C\right)}{1+2\left(\frac{R_C+R_D+R_D R_C G_L)C}{2\sqrt{(1+R_D G_L)(1+R_C G_L)}}\sqrt{\frac{C}{L}}+\frac{G_L}{2\sqrt{(1+R_D G_L)(1+R_C G_L)}}\sqrt{\frac{L}{C}}\right)\frac{s}{\omega_0}+\left(\frac{s}{\omega_0}\right)^2}$$

Comparison with $PTF = \frac{A_0\left(1+s/\omega_{n1}\right)}{1+2\left(D_C+D_L\right)\frac{s}{\omega_0}+\left(\frac{s}{\omega_0}\right)^2} = \frac{A_0\left(1+s/\omega_{n1}\right)}{1+2D\frac{s}{\omega_0}+\left(\frac{s}{\omega_0}\right)^2}$ delivers

$$A_0 = \frac{1}{1+R_W G_L}\xrightarrow{R_W G_L\to 0}1 \qquad \xrightarrow{R_W G_L\to 0} \qquad 1$$

$$\omega_{n1} = \frac{1}{R_C C}$$

$$\omega_0 = \sqrt{\frac{1+R_D G_L}{1+R_C G_L}\cdot\frac{1}{LC}} \qquad \xrightarrow{R_C,R_D,G_L\to 0} \qquad \sqrt{\frac{1}{LC}}$$

$$D_D = \frac{R_D+R_C+R_D R_C G_L}{2\sqrt{(1+R_D G_L)(1+R_C G_L)}}\sqrt{\frac{C}{L}} \qquad \xrightarrow{R_C,R_D,G_L\to 0} \qquad \frac{R_D+R_C}{2}\sqrt{\frac{C}{L}}$$

$$D_L = \frac{G_L}{2\sqrt{(1+R_D G_L)(1+R_C G_L)}}\sqrt{\frac{L}{C}} \qquad \xrightarrow{R_C,R_D,G_L\to 0} \qquad \frac{G_L}{2}\sqrt{\frac{L}{C}}$$

$$D = D_D + D_L \qquad \xrightarrow{R_C,R_D,G_L\to 0} \qquad \frac{R_D+R_C}{2}\sqrt{\frac{C}{L}} + \frac{G_L}{2}\sqrt{\frac{L}{C}}$$

To obtain the quarrel transfer function wa correct DC amplification and add a second zero:

$$QTF(s) = \left.\frac{U_{out}}{-I_L}\right|_{U_{in}=0} = \frac{-R_0\cdot\omega_0^2(1+s/\omega_{n1})(1+s/\omega_{n2})}{s^2+2D\omega_0\cdot s+\omega_0^2}$$

with second pole in $\omega_{n2} = R_D/L$ and DC impedance $R_0 = R_D A_0$